University of Szeged

Faculty of Pharmacy

Institute of Pharmaceutical Technology and Regulatory Affairs

Head: Prof. Dr. Ildikó Csóka Ph.D.

Ph.D. Thesis

DEVELOPMENT OF INNOVATIVE, DOPAMINE PRECURSOR-CONTAINING MICRONIZED POWDER FORMULATIONS BASED ON THE QUALITY BY DESIGN APPROACH

Tamás Kiss

Chemist

Supervisors:

Dr. Gábor Katona Ph.D.

and

Dr. habil Rita Ambrus Ph.D.

SZEGED

2022

PUBLICATIONS RELATED TO THE SUBJECT OF THE THESIS

1. Bartos Cs., Pallagi E., Szabó-Révész P., Ambrus R., Katona G., **Kiss T.**, Rahimi M., Csóka I. (2018) Formulation of levodopa-containing dry powder for nasal delivery applying the quality-by-design approach. EUROPEAN JOURNAL OF PHARMACEUTICAL SCIENCES, 123 475-483. https://doi.org/10.1016/j.ejps.2018.07.061. – IF: 3.532 (in 2018); Q1 Journal

2. **Kiss T.**, Alapi T., Varga G., Bartos C., Ambrus R., Szabó-Révész P., Katona, G. (2019) Interaction studies between levodopa and different excipients to develop coground binary mixtures for intranasal application. JOURNAL OF PHARMACEUTICAL SCIENCES, 108(8), 2552-2560. https://doi.org/10.1016/j.xphs.2019.03.005. - IF: 2.997 (in 2019); Q1 Journal

3. **Kiss T.**, Katona G., Ambrus R. (2021) Crystallization and physicochemical investigation of melevodopa hydrochloride, a commercially available antiparkinsonian active substance. ACTA PHARMACEUTICA HUNGARICA, 91(2) 34-52. https://doi.org/10.33892/aph.2021.91.45-52. - IF: – ; Q4 Journal

4. **Kiss T.**, Katona G., Mérai L., Janovák L., Deák Á., Kozma G., Kónya Z., Ambrus R. (2021). Development of a Hydrophobicity-Controlled Delivery System Containing Levodopa Methyl Ester Hydrochloride Loaded into a Mesoporous Silica. PHARMACEUTICS, 13(7), 1039. https://doi.org/10.3390/pharmaceutics13071039. – IF: 6.321 (in 2020); Q1 Journal

PUBLICATIONS NOT RELATED TO THE SUBJECT OF THE THESIS

1. Baji Á., **Kiss T.**, Wölfling J., Kovács D., Igaz N., Gopisetty M. K., Kiricsi M., Frank, É. (2017). Multicomponent access to androstano-arylpyrimidines under microwave conditions and evaluation of their anti-cancer activity in vitro. JOURNAL OF STEROID BIOCHEMISTRY AND MOLECULAR BIOLOGY, 172, 79-88. https://doi.org/10.1016/j.jsbmb.2017.06.001. – IF: 4.095 (in 2017); Q1 Journal

2. Ambrus R., Szabó-Révész P., **Kiss T.**, Nagy E., Szűcs T., Smausz T., Hopp B. (2020). Application of a suitable particle engineering technique by pulsed laser ablation in liquid (PLAL) to modify the physicochemical properties of poorly soluble drugs. JOURNAL OF DRUG DELIVERY SCIENCE AND TECHNOLOGY, 57, 101727. https://doi.org/10.1016/j.jddst.2020.101727. – IF: 3.981 (in 2020); Q2 Journal

3. Katona G., Balogh G. T., Dargó G., Gáspár R., Márki Á., Ducza E., Sztojkov-Ivanov A., Tömösi F., Kecskeméti G., Janáky T., **Kiss T.**, Ambrus R., Pallagi E., Szabó-Révész P., Csóka, I. (2020). Development of meloxicam-human serum albumin nanoparticles for nose-to-brain delivery via application of a quality by design approach. PHARMACEUTICS, 12(2), 97. https://doi.org/10.3390/pharmaceutics12020097. IF: 6.321 (in 2020); Q1 Journal

4. Gieszinger P., **Kiss T.**, Szabó-Révész P., Ambrus R. (2021). The Development of an In Vitro Horizontal Diffusion Cell to Monitor Nasal Powder Penetration Inline. PHARMACEUTICS, 13(6), 809. https://doi.org/10.3390/pharmaceutics13060809. IF: 6.321 (in 2020); Q1 Journal

PRESENTATIONS RELATED TO THE THESIS

Oral presentations

1. **Kiss T.**, Ambrus R. - Preparation and investigation of levodopa-containing powders for alternative administration. I. Symposium of Young Researchers on Pharmaceutical Technology, Biotechnology and Regulatory Science, Szeged (2019) p. 8., 1 p.

2. **Kiss T.**, Ambrus R. – Treatment of the off-periods of Parkinson's disease with levodopa and its derivative. II. Symposium of Young Researchers on Pharmaceutical Technology, Biotechnology and Regulatory Science, Szeged (2020) p. 40. 1 p.

3. **Kiss T.**, Gieszinger P., Szabó-Révész P., Ambrus R. The investigation of the in vitro penetration of 3 types of model API using modified horizontal diffusion cells, ACTA PHARMACEUTICA HUNGARICA (0001-6659): 90(2-3). Congressus Pharmaceuticus Hungaricus XVI., Debrecen (2020) pp. 92-93. 2 p.

4. **Kiss T.**, Katona G., Mérai L., Janovák L., Szabó-Révész P., Ambrus R. Release Control of Levodopa methyl ester hydrochloride by loading into modified silica. Medical Conference for PhD Students and Experts of Clinical Sciences, Pécs (2020) p.38. 1 p.

5. Ambrus R., Bartos Cs., Katona G., **Kiss T.**, Aigner Z., Szabó-Révész P. – Cyclodextrins in traditional and alternative drug formulations. Proceedings of The 1st International Electronic Conference on Pharmaceutics, online (2020) pp. 8912-8918. 7 p.

6. **Kiss T.**, Katona G., Ambrus R. – Modifying the release of an antiparkinsonian drug by using mesoporous carrier. III. Symposium of Young Researchers on Pharmaceutical Technology, Biotechnology and Regulatory Science, Szeged (2021) p. 15. 1 p.

Poster presentations

1. Bartos Cs., Szabó-Révész P., Rahimi M., Katona G., **Kiss T.**, Ambrus R. – Application of dry milling technique in order to prepare intranasal powder with nanonized levodopa. ACTA PHARMACEUTICA HUNGARICA (0001-6659): 87(3-4) Paper P2B-7. 7th BBBB International Conference on Pharmaceutical Sciences, Balatonfüred (2017)

2. Katona G., **Kiss T.**, Jójárt-Laczkovich O., Szabó-Révész P., Bartos Cs. – Preformulation studies of levodopa containing nasal powders prepared by dry-milling. 11th World Meeting on Pharmaceutics, Biopharmaceutics and Pharmaceutical Technology, Granada (2018) p. 155. 1 p.

3. **Kiss T.**, Alapi T., Varga G., Szabó-Révész P., Katona G. – Physicochemical examination of co-milled levodopa containing nasal powders. ACTA PHARMACEUTICA HUNGARICA (0001-6659): 88(3) Paper P3/6. 12th Central European Symposium on Pharmaceutical Technology and Regulatory Affairs, Szeged (2018) pp. 135-136. 2 p.

4. **Kiss T.**, Katona G., Szabó-Révész P., Ambrus R. – Optimization of co-grinding procedure to prepare levodopa-containing binary nasal powders. Medical Conference for PhD Students and Experts of Clinical Sciences, Pécs (2018) p.10. 1 p.

5. **Kiss T.**, Katona G., Ambrus R. Polymorph screening of an antiparkinsonian drug. EUFEPS Annual Meeting 2021, online (2021) pp. 87-88. 2 p.

6. **Kiss T.**, Katona G., Mérai L., Janovák L., Ambrus R. Investigation of surface modified mesoporous silicas loaded with an antiparkinsonian active substance. 13th Central European Symposium on Pharmaceutical Technology, Gdańsk (2021) p. 113. 1 p.

ABBREVIATIONS

API	Active pharmaceutical ingredient
BBB	Blood-brain barrier
α-CD	α-cyclodextrin
CH	Chitosan
CMA	Critical Material Attribute
CPP	Critical Process Parameter
CQA	Critical Quality Attribute
DSC	Differential scanning calorimetry
EMA	European Medical Agency
FDA	Food and Drug Administration
GC	Gas chromatography
HPLC	High performance liquid chromatography
HPMC	Hydroxypropyl methylcellulose
ICH	The Internation Council for Harmonisation of Technical Requirements for Pharmaceuticals for Human Use
IRR	Initial release rate
LD	Levodopa
LDME	Levodopa methyl ester hydrochloride/melevodopa hydrochloride
LRMC	Levodopa-related motor complication
MAN	D-amnnitol
MPS	Mesoporous silica
NaHA	Sodium hyaluronate

PMDA	Pharmaceutical and Medical Devices Agency
PD	Parkinson’s disease
PVA	Poly(vinyl alcohol)
PVP	Polyvinylpyrrolidone
QbD	Quality by Design
QTPP	Quality Target Product Profile
RA	Risk Assessment
SEM	Scanning electron microscopy
SYL-0	Syloid® XDP 3050
SYL-1	Hydrophobized SYL-0 with 10 mM TMCS
SYL-2	Hydrophobized SYL-0 with 20 mM TMCS
SYL-0	Summary abbreviation of SYL-0, SYL-1 and SYL-2
TMCS	Trimethylchlorosilane
XRPD	X-ray powder diffractometry

TABLE OF CONTENTS

1. INTRODUCTION

Dopamine precursors – such as levodopa (LD) and levodopa methyl ester hydrochloride (LDME) – are considered first-line treatments for Parkinson's disease (PD). The LDME tends to convert to LD in the peripheral circulation, which can pass through the blood–brain barrier (BBB) into the central nervous system, where it converts to dopamine [1]. It can compensate for the dopamine deficiency, the major consequence of PD leading to the improvement of the symptoms. There is only one LDME-containing effervescent tablet available on the Italian market under the name of Sirio® (Chiesi Farmaceutici SpA, Parma, Italy) which utilizes the high solubility of the drug [2]. The LD-containing formulations are more widespread, they are mostly taken orally as a tablet but both intestinal gels [3] and a pulmonary powder [4] are also available on the market. Oral LD administration leads to *off* periods which can be grouped into three main types: *wearing off*, *delayed o*n and *no on* periods [5]. As they develop because of different pharmacokinetic reasons, they demand different formulation strategies.

The preparation of novel, innovative dosage forms, like microparticles, becomes more and more remarkable because they might have improved pharmacokinetic properties owing to controlling the drug release. Microparticles can be formulated in two ways: by either bottom-up or top-down techniques. The top-down techniques can mean milling or grinding of the material which is an easy-to-control method [6]. The co-milling of an active pharmaceutical ingredient (API) with an excipient is beneficial because the microparticles can reduce the particle size of each other. Mesoporous materials, like mesoporous silica (MPS), can be loaded with drugs resulting in an amorphous state [7]. Thus, the release can be controlled by the surface properties of the matrix and the API-matrix interactions.

The significance of alternative delivery routes (intranasal, pulmonary) has a high impact nowadays. The nasal formulations can provide a higher bioavailability compared to oral drug delivery due to avoidance of the hepatic first-pass effect, short onset and high extent of vascularization. On the other hand, short residence time, low permeability in the case of hydrophilic drugs, stability issues and limited dose must be taken into consideration [8]. Most of these issues can be managed by using nasal powders instead of liquid dosage forms. The intranasal delivery of a dopamine precursor API can be used as an emergency complementary treatment besides the oral one to reduce the *delayed on* periods. The oral dosage forms are well-explored but the release prolongation of a dopamine prodrug can reduce the *wearing off* periods.

2. AIMS OF THE WORK

This Ph.D. work aimed to prepare novel, innovative dopamine prodrug (LD, LDME)-containing micronized solid intranasal and oral dosage forms which can be used as a substitution or a complementary therapy to the conventional oral LD administration via controlling the drug release. The research work was planned to construct according to the following steps:

I) A detailed literature review was planned to find the unexplored areas in the literature on the field of development of dopamine prodrug-containing formulations for alternative and conventional drug delivery.

II) Using the results of the detailed literature review and the pre-experiments of LD- and LDME-containing micronized systems, the Quality Target Product Profile (QTPP), the Critical Quality Attributes (CQAs) and the Critical Process Parameters (CPPs)/Critical Material Attributes (CMAs) were intended to define in order to construct efficient experimental designs for both nasal delivery of LD and oral delivery of LDME according to the principles of Quality by Design (QbD) approach.

III) The nasal powders were planned to prepare by co-milling binary powder mixtures comprising LD and an excipient with either mucoadhesive, absorption enhancer or humectant properties according to an experimental design to optimize the physicochemical and pharmaceutical technological properties. A further aim was the prioritization of the products based on mean particle size, crystallinity, *in vitro* drug release rate and stability to prepare stable formulations with immediate release.

IV) The research also aimed to prepare LDME-containing hydrophobized MPSs for oral administration. In this part of the work, the purpose was to prepare stable formulations with zero-order drug release kinetics and extended release according to an experimental design that was determined on QbD basis. We planned to evaluate the effect of hydrophobization extent and drug loading into a silica carrier on physicochemical properties, stability and *in vitro* drug release. Our plans also included the investigation of the LDME properties crystallized from different solvents to discover presumable polymorph forms.

V) After evaluation of the results of the optimization process, we intended to suggest optimized nasal and oral formulations, which are potentially capable of reducing the *delayed on* or *wearing off* periods.

3. LITERATURE BACKGROUND OF THE RESEARCH WORK

3.1. The treatment of PD with dopamine precursors

PD is one of the most widespread neurodegenerative diseases all over the world. During the progress of the disease, the level of dopamine decreases because the *substantia nigra* is damaged [9]. The neurons are unable to transmit messages, causing the three main symptoms of PD: tremor, rigidity, and bradykinesia [10]. Genetic and environmental factors also play a role in its development.

At this moment, the disease is mostly treated by replacing the missing dopamine. As dopamine degrades quickly, dopamine prodrugs are required in the therapy, like LD and LDME (Figure 1.). In the oral therapy , the LD is absorbed in the duodenum but its bioavailability is exceedingly low and fluctuates because of the erratic gastric emptying [11]. The fluctuating active transport depends on the protein content of the food (LD attaches to the L-amino acid carrier) and the strong first-pass effect in the liver. Around 1 % can reach the brain due to the peripheral decarboxylation by DOPA-decarboxylase in the blood [12]. High doses should be applied; therefore the presence of peripheral dopamine can also lead to undesirable side effects. A standard clinical solution to reduce the peripheral decarboxylation is the co-administration of DOPA-decarboxylase inhibitors, like carbidopa and benserazide. Thus, the required dose can be reduced by 75 %. The chemical structure of inhibitors is similar to LD. The LD-containing tablets usually contain 50-250 mg of API. The LD-containing formulations are mostly on the market as oral immediate release tablets and capsule dosage forms [13,14].

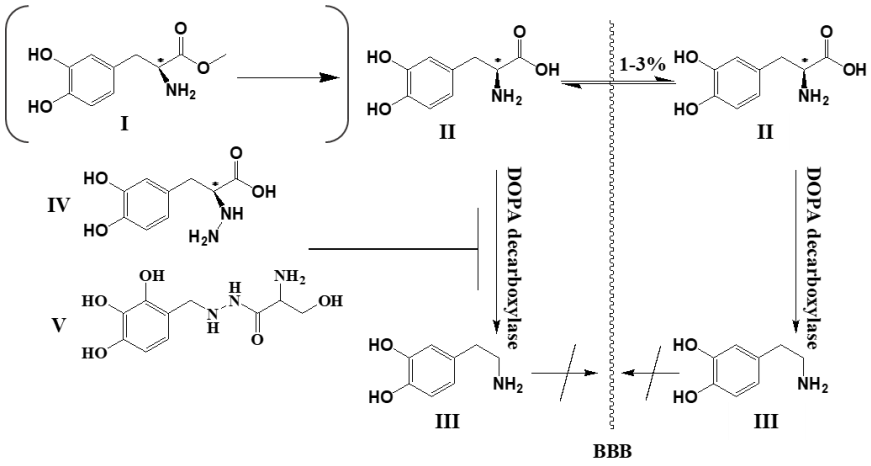

Figure 1. The LDME-LD and LD-dopamine conversion and the short summary of LD pharmacokinetics; I) LDME, II) LD, III) dopamine, IV) carbidopa, V) benserazide

In the early stage of the treatment, the LD is effective because the preserved capacity of presynaptic neurons is high, therefore the LD can be stored, causing a long period in the therapeutic range [15]. As the conventional LD therapy progresses, the therapeutic interval (*on time*) becomes narrow and the blood level becomes unpredictable, causing side effects, called LD-related motor complications (LRMCs) [16,17] resulting in the so-called *on-off* phenomenon [18] (Figure 2.) When the LD concentration is under the therapeutic range, it is called the *off period* which has three main subtypes. As PD advances, there is a remarkable loss of neurons, which reduces the half-time of LD (*wearing off*). Another type is called *delayed-on* which occurs because gastric emptying is often delayed. The blood level of LD does not necessarily achieve the therapeutic range (*no-on*), which can be considered an extreme form of *delayed-on* [19]. The erratic drug absorption also needs to be improved to treat the *off* periods. Approximately 50 % to 80 % of patients with PD experience LRMCs after 5 to 10 years of LD treatment [20]. Pharmaceutical preparations, which aim to treat the *off* periods, can be divided into two groups: either a ”rescue” formulation comprising quick onset [21] as a complementary treatment for the *delayed on* phenomenon or a different strategy includes making a formulation that provides a steady blood level for longer motor control to treat the *wearing off* periods [3].

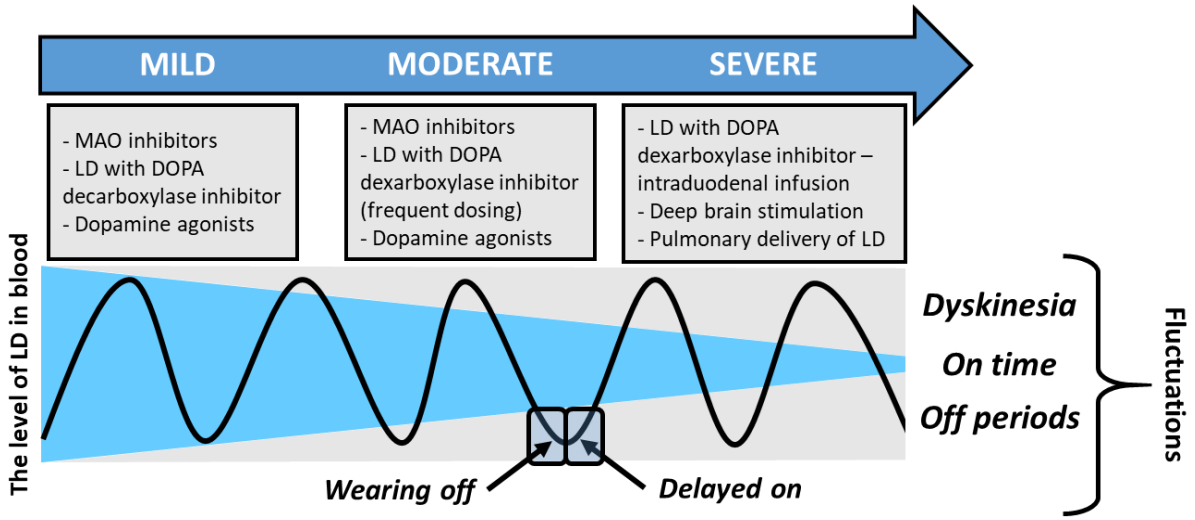

Figure 2. The progress of PD [22,23]

When the disease becomes severe, it can be treated in alternative ways, like - among others - the pulmonary delivery or duodenal infusion of LD, therefore it is an important goal in pharmaceutical technology to improve motor control. Sinemet CR® was the first improvement in contrast to the traditional immediate release tablets, which comprised LD-containing

controlled release formulation for the first time. To reduce the onset, a sublingual formulation, Parcopa® was developed. Besides, Rytary® is also available on the market with both immediate release and delayed release properties [24].

Regarding the alternative delivery routes, intraduodenal infusion of LD/carbidopa gel (Duodopa; Solvay Pharmaceuticals, Allschwil, Switzerland) is commercially available for the treatment of severe PD. It can provide much more *on* time but it is invasive [17,25]. Besides, based on the consept of "quick onset", both the Food and Drug Administration (FDA) [26] and the European Medical Agency (EMA) [27] approved a non-invasive, pulmonary dry powder inhalation system (Inbrija®; Acorda Therapeutics, Inc., Ardsley, USA) whose therapeutic effect occurs within 10 min [28]. Deep brain stimulation can also improve the well-being of patients with severe PD.

Furthermore, clinical studies claim that oral LD-containing liquid formulations have greater bioavailability than solid tablets [29,30]. One of the limitations of LD formulations is the low solubility, which slows down the dissolution, therefore intensive research was carried out to find more soluble derivatives of LD in the last decades. The ester prodrugs seem quite promising, among which the LDME is the most studied [12]. The LDME is around 250 times more soluble than the LD, and consequently high doses can be prepared in liquid formulations [2]. Its ability of absorption is also higher due to its higher lipophilicity. On the basis of the molecular weight ratio, 1.256 mg of LDME is equivalent to 1.000 mg of LD [2,29]. Only one polymorph of both LD and LDME is known according to the Cambridge Crystallographic Data Centre [31]. The LDME is marketed as an effervescent tablet under the name of Sirio® in Italy (Chiesi Farmaceutici SpA, Parma, Italy). The advantage of the effervescent tables is that the resulting liquid passes more easily through the stomach, thereby the erratic gastric emptying effect is lower causing quicker onset. Thus, the *delayed on* periods might be reduced in patients with advanced PD compared to LD-containing tablets [32]. In the clinical trials, the Sirio® was found to have a more reliable pharmacokinetic profile with less drug accumulation and less variability than the standard LD/carbidopa formulations which resulted in reduced LRMCs. Based on the favourable properties of the LDME, some articles studied alternative administration opportunities but there is still a lack of information on this field despite some promising results. South Korean researchers found higher bioavailability and clearance of formulated LDME-containing nasal powder compared to oral LD in rats, additionally, the time

to maximum concentration was lower [33]. Meanwhile, the nasal dose was lower (15 mg/kg) than the oral dose (80 mg/kg). As the LDME solubility in aqueous media is very high, the control of its release rate is a technological challenge. The LD and LDME are unstable in aqueous solutions, therefore the formulation of solid dosage forms is preferable to the liquid forms.

3.2. Intranasal drug delivery

The surface area of the nasal cavity is around 160 cm^2. The nasal cavity can be divided into three parts: the nasal vestibule, the respiratory region and the olfactory region. The penetration of drugs into the central nervous system occurs mainly through the respiratory region [34]. After the drug enters the bloodstream, it can reach the central nervous system through the BBB avoiding the hepatic first-pass effect [35]. Besides, the olfactory region can also be a key area as it provides a direct nose-to-brain delivery opportunity by the axonal transport bypassing the BBB. The axonal transport can be realized through mass flow and diffusion in perineural channels, perivascular spaces, or lymphatic channels in direct contact with brain tissue or cerebrospinal fluid, however, an accurate explanation does not exist yet [36].

The outer surface of the nasal epithelial cells contains constantly moving cilia in the direction of the pharynx eliminating any exogenous particles which phenomenon is called mucociliary clearance with a half-life of about 15 min in the case of healthy adults [37]. For this reason, the residence time means a limitation for the nasal formulations.

3.2.1. The significance of nasal formulations nowadays

In the European Pharmacopeia nasal drops, nasal sprays, nasal powders and semi-solid products are listed for nasal administration [38]. When planning a formulation strategy, the following factors must be taken into consideration: local or systemic delivery, single dose or repetitive administration, the dosage, the solubility of the drug, the stability of the drug and toxicity [39]. The nasal formulations have high bioavailability because of the avoidance of the hepatic first-pass effect and the high vascularization of the nose and low onset, besides, the direct nose-to-brain delivery can also be important in the case of dopamine precursors. In the future it can become a non-invasive alternative to intravenous administration with higher patient compliance. On the other hand, the limited residence time, the stability of the liquid formulations, the low permeability of hydrophilic drugs and molecules with high molecular weight, as well as the limited dose should be managed [40,41]. The residence time can also be

increased with the help of a highly viscous environment (mucoadhesive excipients are also preferred).

The stability can be improved with stabilizers and absorption enhancers can help to accelerate the absorption. Additionally, the solubility enhancers can increase the solubility of the API. All of the limiting factors might be improved by using nasal powders [41] (Figure 3.).

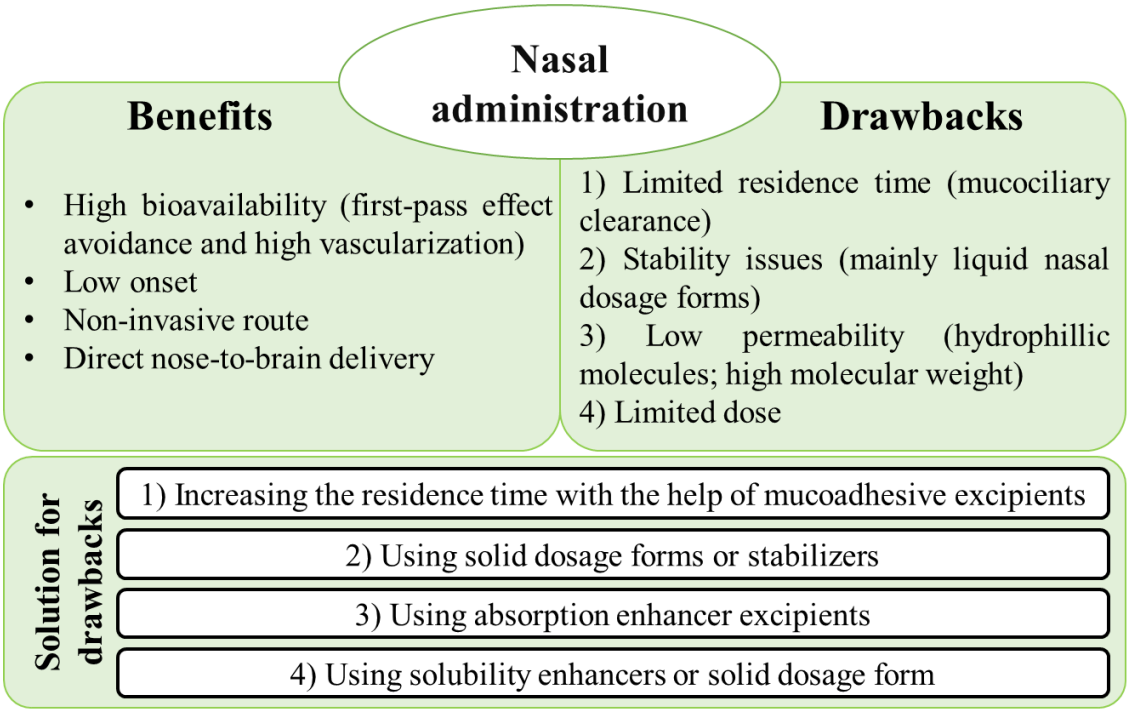

Figure 3. The benefits and drawbacks of nasal administration, as well as the possible solutions to minimize the drawbacks

The excipients in the nasal drug delivery can be grouped into the following way [41]:

- Absorption enhancers: they open the tight junctions (cyclodextrins, polysorbate 80).
- Mucoadhesive agents: they have a synergistic effect with the mucin (poly(vinyl alcohol) (PVA), poly(vinylpyrrolidone) K25 (PVP), hydroxypropyl methylcellulose (HPMC), chitosan (CH), sodium hyaluronate (NaHA)).
- Fillers: they can have an impact on the dissolution and absorption (mannitol, sorbitol).

On the other hand, the excipients can also exhibit unexpected side effects on the performance of the formulation, which can be both advantageous and disadvantageous. An advantageous or neutral effect on the desired properties of the formulation is called compatibility, whereas a disadvantageous effect on the desired properties of the formulation is called incompatibility.

As a consequence, drug-excipient compatibility studies are essential [42]. These effects can be influenced by either the secondary interactions between the API and the excipient (the excipient might also affect the stability), the physicochemical properties of the additive, the behaviour of the excipient during dissolution, its effect on the biological membrane or the biocompatibility. The LD shows interactions with numerous additives like calcium-lactate, magnesium-stearate, lactose, talcum and silica [43].

The nasal powders are and widespread than the liquid formulations despite their advantages, like high applicable doses, stability, increased residence time and possible absorption enhancement. Only a few nasal powders are commercially available [38,44] (Table 1.).

Table 1. The commercially available nasal powders [41,45–47]

Product name:	**Tejin Puvlizer Rhinocort®**	**Rhinocort® Turbuhaler®**	**Erizas®**	**Onzetra® Xsail®**	**Baqsimi™**
API:	Beclo-methasone dipropionate	Budesonide	Dexamethasone cipecilate	Sumatriptan succinate	Glucagon
Additives:	HPMC, magnesium stearate, stearic acid	-	Lactose	-	Betadex (E459), dodecyl-phosphocholine
Device:	Single-dose patient-operated capsule-based device	Multi-dose breath-actuated metering device	Device for 400 µg: capsule-based breath-actuated Device for 200 µg: multi-dose nasal spray	OptiNose's Bi-Directional Breath Powered™ technology	Unidose System powder device
Indication:	Allergic and vasomotor rhinitis	Seasonal or perennial allergic rhinitis	Allergic rhinitis	Migraine	Severe hypoglycaemia (with short onset)
First approval*:	PMDA (1986)	FDA (1999)	PMDA (2012)	FDA (2016)	FDA (2019)

*FDA = Food and Drug Administration (authority in the USA); PMDA = Pharmaceutical and Medical Devices Agency (authority in Japan)

Most of the nasal powders were approved by the authorities in the last 11 years showing their increasing relevance, therefore this type of formulation is gaining increasing attention nowadays. There is no scientific consensus regarding the mean particle size of nasal powders, but it is accepted that the mean particle size must be above 5 µm, otherwise a remarkable portion

of powder is expected not to adhere to the mucosa of the upper airways but rather to the lungs [48]. Accordingly, it is crucial to use a nasal powder with a mean particle size (D_{50})> 5 μm, preferably between 5–40 μm [49]. According to other authors, the ideal particle size range is in the range of 10–45 μm [41]. On the other hand, the low particle size can be beneficial due to the quicker drug release. The nose does not exhibit clear particle size cutoffs and deposition appears to be highly affected by the properties of the formulation and administration device [38].

3.2.2. Engineering opportunities of applicable microspheres for nasal formulations

Each manufacturing method is suitable for nasal powder preparation that results in the desired particle size range. The methods can be grouped into bottom-up and top-down techniques.

1) Main bottom-up techniques (the microparticles are built from dispersed particles) [41]:

- Freeze-drying [50]: it is not a widespread technique, because numerous drugs are poorly water-soluble, and the use of organic solvents can result in a lower freezing point; moreover, they might damage some parts of the freeze dryer. The products are often not homogeneous.
- Spray-drying [51]: it is a widely used technique because of the utilizable high concentration range, including the use of suspensions, multiple options for solvent and tuneable parameters (flow rate, pressure, temperature). It allows the optimization of particle size, shape and density of the powder. However, the yield is relatively low because of the material loss and sensitive materials are not allowed to be used.
- Supercritical fluid-assisted spray drying [52]: it is a novel technique, nasal absorption of the particles produced with supercritical fluid-assisted spray drying was higher than in the case of the spray-dried ones.
- Spray freeze-drying [53,54]: it is also a novel technique aiming to combine the advantages of spray-drying and freeze-drying. It consists of a dispersion of liquid into droplets, droplet freezing and drying by sublimation. A few nasal powders have been prepared with this method, however, it can also be preferred for poorly water-soluble drugs over freeze-drying.
- Agglomeration of micronized powder [55–57]: if the particle size is below 100 μm, it can occur spontaneously because of the high surface/volume ratio. This phenomenon can be improved by using binder excipients (like soybean lecithin).

2) Main top-down techniques (miniaturization of materials powders leading to the formation of micro- or nanostructures):

- Milling [58]: it is the action of reducing the size of particles thanks to mechanical action. It is advantageous because organic solvent is not required for this process which makes it an environmentally desirable technology because a limited residual of the organic solvent can remain in the formulations (detailed in the ICH Q3C (R8) guideline [59]). Ball milling is widely used in the pharmaceutical industry because of its simple optimisability (using the rotational speed, milling time and ratio of materials) and its well-explored scalability [60,61].

Co-milling can be a solution to achieve the desired micronized particle size range for nasal drug delivery. During the co-milling, the harder particles might grind the softer particles. In the case of planetary ball mill, the milling balls also grind the particles. This process can lead to microspheres.

3.2.3. Dopamine precursor-containing nasal formulations

As the LD and LDME are chemically unstable, it is advantageous to develop solid dosage forms over liquid formulations. The LD has been prepared as a nasal powder (microspheres) [62] or nasal gel [63] (including *in situ* gelling systems [38,64]) for the same purpose as in some cases in the literature, i.e. to treat the *delayed on* periods as complementary therapy but there is still a huge amount of missing information on this field.

The *ex vivo* intranasal permeation of solid LD was compared with that the permation of dissolved LD through the freshly excised bovine olfactory mucosal membrane. The study has shown that the LD powder was more stable and the average steady-state flux was higher than the dissolved LD, which probably occurred due to a higher steady-state concentration gradient of powder. These authors sieved the LD powder and collected a fraction whose average particle size was around 20 μm, however, the nasal powder did not contain an excipient which could have improved the performance [65]. According to *in vivo* comparison of nasal and oral delivery of LD, the onset of nasal formulation and the area under curve value were lower, the maximum concentrations were similar [66]. However, the LD was dissolved before the experiment, which could reduce bioavailability compared, as presented by the above-mentioned *ex vivo* results [65].

Besides, an LDME powder-containing “nasal powder” formulation was prepared by mixing the LDME with different excipients (N-acetyl-L-cysteine, 2-hydroxypropyl-ß-cyclodextrin, silicated microcrystalline cellulose, Carbopol 974 P, hydroxypropyl cellulose, carboxymethyl cellulose sodium) but the particle size of the formulations was not optimized. In this article,

LDME-containing nasal powders were prepared and investigated *in vitro* [67]. Thereafter, the LDME was compared to oral LD *in vivo* in male Sprague–Dawley rats. The LDME-containing nasal powders exhibited lower onset than the oral LD. Based on the results, LD and LDME could be proper therapy of *delayed on* periods [33,66].

3.3. The use of MPSs as excipients – oral delivery

Silica-based (SiO_2) materials play a key role in the lots of application fields, for instance, in chromatography, catalysis and adsorbents [68,69]. The preparation of amorphous solid dispersions has become widely applied recently because a system with similar features to solutions can be achieved by making the incorporated material amorphous [7,70]. MPS is an excellent matrix material candidate for both immediate and extended release drug delivery systems. Their pore diameter is between 2–50 nm. They have high pore volume and specific surface area to adsorb the required amount of API in the matrices. The silanol-containing surface implies the ability to be functionalized to allow better control of drug absorption and loading [70,71]. As a result of drug loading, the adsorbed API becomes amorphous in the mesopores. Thereafter, the recrystallization is inhibited, which can be explained by two mechanisms [72]:

1) as secondary interactions are developed between the drug and the groups on the silica surface, therefore the free energy of the amorphous adsorbed material is lower than the crystalline;

2) the critical crystalline nucleus of the drug is larger than the mesoporous diameter thereby inhibiting the nucleus growth.

The release rate of the API cannot be only accelerated with amorphization in an MPS but it can also be prolonged. Lots of articles focus on the immediate release of water-insoluble drugs but achieving extended release of water-soluble APIs has been conducted with the help of MPS surface modification only by some authors. The dominant functional groups of silica are siloxane (Si-O-Si) and silanol (-Si-OH) groups. Due to the hydrophilic groups the MPS can adsorb a remarkable amount of water. The drug release and absorption can be tuned with the help of the functionalization of the silanol groups [70,71,73]. It can mean functional groups on the modified surface which develop strong interactions with the drug retarding the release rate. In the case of different approach, the drug-surface interactions are not necessarily increased but the aqueous wettability of the silica derivative is decreased, therefore the aqueous medium penetration is decelerated resulting in controlled drug release [74–76]. The wettability of finely

divided materials can be studied with numerous methods among which the contact angle measurement is still the most spread and a widely accepted method. A strong tool for hydrophobization reaction is by silylation with trimethylchlorosilane (TMCS) [75].

Aside from the surface-water/surface-drug interactions, the structural properties also influence the behaviour of MPSs. The pore structure in the MPSs can be ordered and non-ordered depending on the synthesis method [77]. The pore size is proportional to the amount of loaded drug but as the width of pores and/or the amount of incorporated drug increases, the chance of recrystallization will also increase. The release speed is proportional to the specific surface area if the adsorbed API is in monolayer format but if it is in multilayer form, the release rate is inversely proportional to the pore volume and inversely proportional to the pore length [70].

The drug loading/incorporation into MPSs can be grouped into solvent-free and solvent-based methods [78]. The solvent-based methods are more widespread, they are presented in two steps: preparation of an MPS suspension in a solvent that can dissolve the drug molecule in high concentration and subsequent removal of the medium. The solvent removal can be carried out by filtering the solid dispersion (immersion method) or evaporation (spray drying, solvent drying, supercritical fluid and incipient impregnation method) [71,77]. The dissolution of API and the solvent evaporation steps can be repeated to achieve a higher loading extent. Although, the immersion method is the most widespread, a higher loading extent can be reached with the solvent drying method [79,80]. During the popular solvent drying method, the MPS suspension is stirred for a well-defined time, then it is evaporated with a rotary evaporator or rotavapor. As the evaporation of the loading solution occurs, a concentration gradient develops and the drug incorporation is initiated into the pores. This method is preferred because a high API amount can be loaded into the MSPs. In our literature, we could not find an article dealing with loading LDME into the pores of a MPS.

Among the MPSs, only limited studies can be found in connection with hydrophobized Syloid® based drug delivery systems [81,82]. Nevertheless, these formulations have a highly developed mesoporous network and a large surface area, therefore a high amount of drug can be absorbed on the surface. In the literature, the MPSs were mainly used to enhance the dissolution of poorly water-soluble drugs [79,81,83,84], the control of drug release with surface-modified MPS is a less studied area [85]. The Syloid® XDP 3050 (SYL-0) is a known type of Syloid® based matrices (Table 2.).

Table 2. Specification of Syloid® XDP 3050

Mean particle size (µm)	Shape	Specific surface area (m^2/g)	Pore volume (cm^3/g)	Pore diameter (nm)
50	Irregular	287	1.69	22.9

Besides, their application is safe, the No Observed Adverse Effect Level of orally administered Syloid® 244 was high, 9000 mg/kg body weight/day in rats with exposure of 90 days initiating safety [86]. Dopamine precursors had not been loaded into the pores of Syloid® excipient.

3.4. The QbD approach

The QbD was replaced the Quality by Testing quality approach which meant that there was a fixed system and the compliance ranges were narrow. For this reason, the execution of processes was crucial: otherwise, the different input parameters led to different products. In contrast to that, the QbD approach allows the change of input parameters in a predetermined specification range [87]. The QbD is a holistic, systematic, knowledge- and risk-based quality management system and pharmaceutical development model. It tries to incorporate expectations into the product already at the design stage, for which it requires an accurate, pre-determined definition of the product. The formulation and manufacturing processes are designed and developed to provide predetermined product specifications [88].

The concept of QbD was first outlined in 1992 by a quality management consultant called Joseph M. Muran [89]. The Juran trilogy:

- Quality planning: defining and assessing customer needs, "customer focus";
- Quality management: to plan the process for the purpose, to ensure its quality;
- Quality improvement: control, feedback, organization development.

Based on the approach, outlined by Muran, the Food and Drug Administration (FDA) published a report in 2002 entitled “Pharmaceutical Quality for the 21st Century A Risk-Based Approach Progress Report” and adopted these principles in 2004. The International Council for the Harmonization of Technical Requirements for Pharmaceuticals for Human Use (ICH) has also adopted this approach. QbD is detailed in ICH Q8 (Pharmaceutical Development) [90], ICH Q9 (Quality Risk Management) [91] and ICH Q10 (Pharmaceutical Quality System) [92].

4. MATERIALS AND METHODS

4.1. Materials

4.1.1. The active pharmaceutical ingredients (APIs)

Levodopa (LD) was obtained from Hungaropharma Ltd. (Budapest, Hungary), levodopa methyl ester hydrochloride/melevodopa hydrochloride (LDME) (Table 3.) was bought from the Merck Ltd. (Darmstadt, Germany).

Table 3. The physicochemical and pharmaceutical properties of the dopamine prodrug APIs

Dopamine prodrug	**Levodopa (LD)**	**Levodopa methyl ester hydrochloride/Melevodopa hydrochloride (LDME)**
Chemical structure	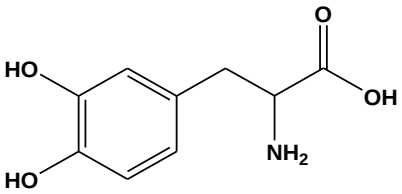	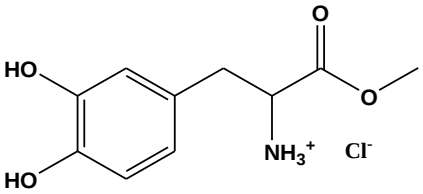
Chemical name	L-3-(3,4-dihydroxy-L-phenyl)alanine	L-3-(3,4-dihydroxyphenyl)alanine methyl ester hydrochloride
Physical properties	White crystalline powder	Elongated crystals, white powder
Stability	Stable at room temperature, unstable in aqueous solutions, stable at low pH [93]	Unstable in solution, stable at low pH, the main degradation product is LD [67,94]
Storage	At room temperature	In a freezer (-20 °C)
Solublity in water	5 mg/ml [14]	912 mg/ml [95]
logP	-2.9 [96]	0.64 [97]
M_w	197.19 g/mol	247.67 g/mol
Site of action	LD and LDME are prodrugs of dopamine, they are needed because the dopamine degrades quickly in the body. In the brain, LD is decarboxylated to dopamine by DOPA decarboxylase and stimulates the dopaminergic receptors, thereby compensating for the depleted supply of endogenous dopamine [98].	

4.1.2. Excipients and other materials

Chitosan (M_w = 3,800 – 20,000 Da) (CH), α-cyclodextrin (α-CD), METHOCEL™ K4M hydroxypropyl methylcellulose (HPMC), poly(vinylpyrrolidone) K25 (PVP), poly(vinyl alcohol) ($M_w \approx$ 24,000 Da) (PVA) and D-mannitol (MAN) were obtained from Merck Ltd. (Darmstadt, Germany). Sodium hyaluronate (NaHA) (M_w = 1,400 kDa) was received as a gift from Gedeon Richter Plc. (Budapest, Hungary). Syloid® XDP 3050 (SYL-0) was manufactured and kindly provided by Grace Materials Technologies (Grace GmbH, Worms, Germany) (Table 4.).

For LDME-loaded MPSs, *n*-hexane and trimethylchlorosilane (TMCS) were purchased from Merck Ltd. (Darmstadt, Germany).

For buffer preparation, hydrochloride acid, monosodium phosphate, potassium dihydrogen orthophosphate and 85 % w/w phosphoric acid were also obtained from Merck Ltd. (Darmstadt, Germany). Potassium hydroxide and methanol were purchased from VWR International Ltd. (Radnor, PA, USA).

Table 4. The used excipient in the Ph.D. work, their structural formula and role in drug delivery (advantageous pharmaceutical technological properties)

Excipient	Structural formula	The role in drug delivery
CH	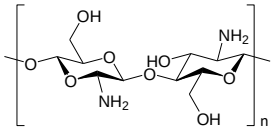	Mucoadhesive material Absorption enhancer [99,100]
NaHA	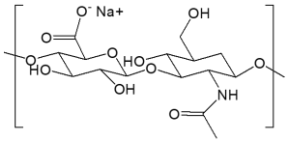	Mucoadhesive material [101]
α-CD	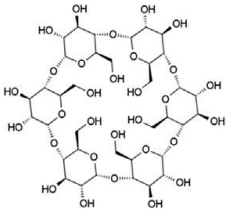	Absorption enhancer [37,102,103]
HPMC	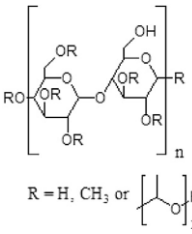	Mucoadhesive material Gel forming agent [104]
PVP	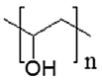	Mucoadhesive material [105]
PVA	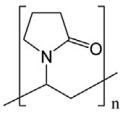	Mucoadhesive material [106]
MAN	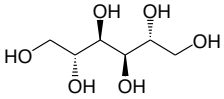	Humectant [107]
SYL-0	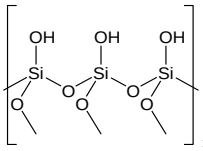	Mesoporous silica (MPS) Proper for drug loading and amorphization Insoluble in water [7]

4.2. Methods

4.2.1. The QbD approach for the development of formulations

The first step of pharmaceutical development with the help of the QbD approach involves the retrospective determination of the QTPP of the target product. These properties of the product from the aspect of therapeutic use (indication, efficacy, safety, route of administration, sterility, stability, etc.). It is directly influenced by the CQAs of the products, i.e. the physical, chemical and microbiological properties that influence the safety and efficacy of the product, which are appropriate in a certain range. The next step is to develop the knowledge space, which can be used to define the critical factors (production process parameters and the characteristics of the starting materials) that have a decisive influence on our production process or the properties of the products so that the process is optimized to produce a product with the appropriate CQAs. Thus, the production parameters: CPPs and the properties of the starting API(s) and excipient(s): the CMAs should be defined (Figure 4.). This process is called Risk Assessment (RA). During the RA, we also take severity, occurrence, or uncertainty of the given risk into account to establish a priority order among the CQAs directly influencing the QTPP and the CPP/CMAs directly influencing the CQAs, i.e. the CPP/CMAs can be used to indirectly control the QTPP. Several quality tools can be used for knowledge space development and RA, such as Ishikawa diagram, flowchart, decision tree, Pareto diagram and so on. The QbD approach can be applied for formulations of both nasal [108,109] and oral delivery [110,111].

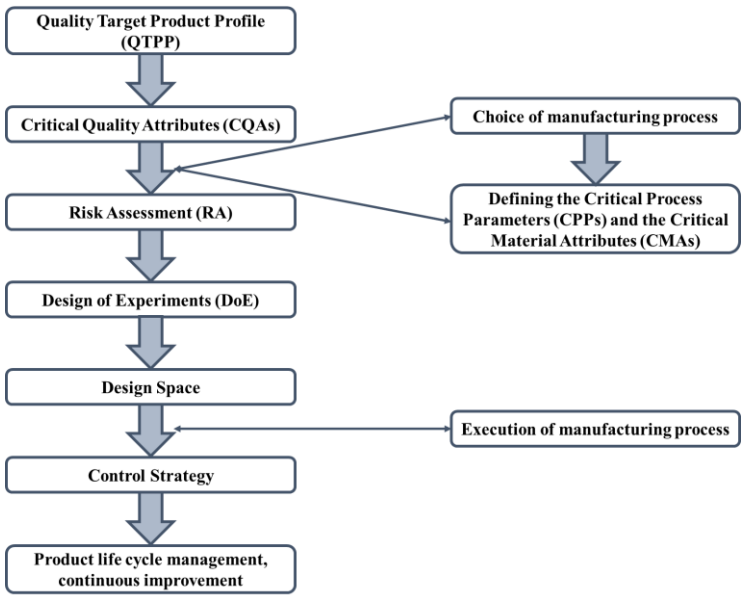

Figure 4. The elements and steps of the QbD approach on a flow chart

4.2.2. Co-milling of LD-containing binary mixtures

2.00 g of LD-excipient binary mixtures were co-ground (Table 5.) in a planetary ball mill (Retsch PM-100 MA, Retsch GmbH, Haan, Germany) for a maximum of 90 min using 10 stainless steel milling balls with a diameter of 8 mm (Figure 5.) in a 50 ml milling chamber, the mean particle size was determined with laser diffraction (Malvern Mastersizer Scirocco 2000; Malvern Instruments Ltd., Worcestershire, UK). The LD-excipient combinations were selected for more detailed analysis which satisfied the requirements of particle size and crystallinity.

Table 5. The excipients used to formulate binary nasal powders with LD and the parameters of experimental design constructed based on the QbD-based initial RA

Excipient	Drug: additive mass ratio	Milling time (min)	Rotational speed (rpm)
CH	50:50; 66.67:33.33	60; 90	300; 400
NaHA			
α-CD	30:70; 50:50; 70:30	15; 30; 45; 60	400
HPMC			
PVP			
PVA			
MAN			

The goal of the optimization regarding the D_{50} value was to reach the 5-40 μm range. As a result of co-grinding, LD-excipient microparticles were formed and due to the mechanical impact, interactions could be formed between the materials.

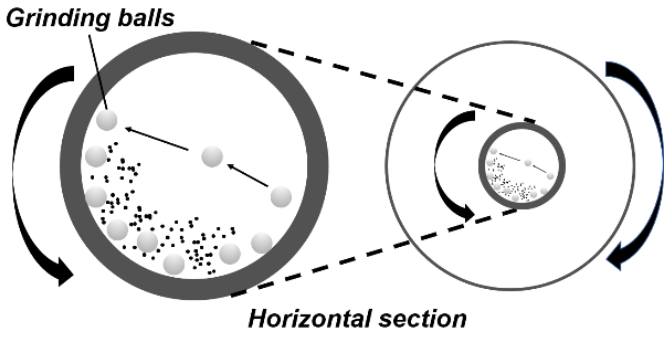

Figure 5. The working principle of the planetary ball mill

4.2.3. The hydrophobization of the MPS

Experimental results reported in the literature showed that water plays a key role in the silylation reactions [112], therefore the adsorbed water content of the silica surface needed to be standardized before the reaction. The adsorbed water content of SYL-0 was standardized in a climate chamber (KKS TOP+, Wodzisław Śląski, Poland) at 40 °C and relative humidity of 75 % for at least 3 days to reach the equilibrium. The silylation reaction was performed at 25 °C. 200 mg of SYL-0 was dispersed in 20.0 ml of *n*-hexane in a pre-hydrophobized capped glass vial with a volume of 40 ml. TMCS was added to the dispersion at a concentration of 10 mM (to provide the SYL-1 derivative with moderate aqueous wettability) or 20 mM (to provide the SYL-2 derivative with poor aqueous wettability). The reaction mixtures were stirred by magnetic stirring bars at 700 rpm for 2 hours, then the solids content was obtained through filtration on a regenerated cellulose membrane with a pore size of 0.45 μm (Whatman™, GE Healthcare Sciences, UK) and the washing with 3×15 ml of *n*-hexane. The reaction mechanism is summarized in Figure 6.

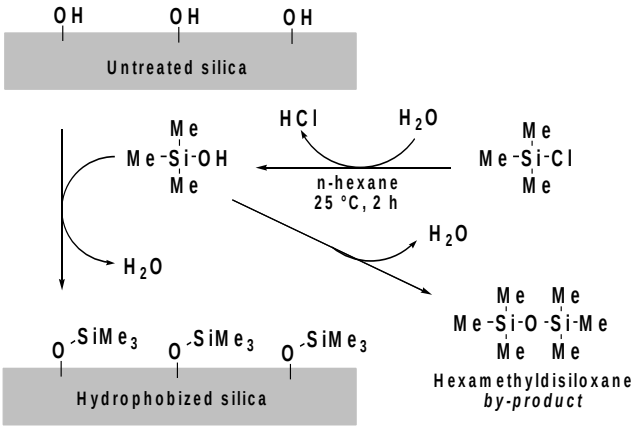

Figure 6. Mechanism of silica hydrophobization via TMCS

4.2.4. Loading of the MPS

For the loading process, a BÜCHI Rotavapor R-125 equipment (BÜCHI Labortechnik AG, Flawil, Switzerland) was used (Figure 7.). A certain amount of LDME (m_{LDME}=25.0 or 62.5 or 100 mg) was dissolved in 5.00 ml of methanol in a round-bottom flask. Thereafter, SYL-0, SYL-1, or SYL-2 was dispersed in the solution according to the planned SYL:LDME mass ratio in the products (see Table 6.).

Table 6. The 3^2 full-factorial design constructed based on the QbD-based initial RA to prepare SYLs loaded with LDME

c_{TMCS} (mM)	LDME:SYL mass ratio	Abbreviation: SYL-X-Y
0	5.00:95.0	SYL-0-5
	12.5:87.5	SYL-0-12.5
	20.0:80.0	SYL-0-20
10.0	5.00:95.0	SYL-1-5
	12.5:87.5	SYL-0-12.5
	20.0:80.0	SYL-0-20
20.0	5.00:95.0	SYL-2-5
	12.5:87.5	SYL-2-12.5
	20.0:80.0	SYL-2-20

The sum of the mass of the dissolved LDME and dispersed SYL was around 500 mg in each case. Methanol was evaporated at 50 °C and 135 mbar pressure. The applied rotation speed was 120 rpm. Due to the rotation, the dispersion remained homogenous during the process. The resulting dry powder was stored in a freezer.

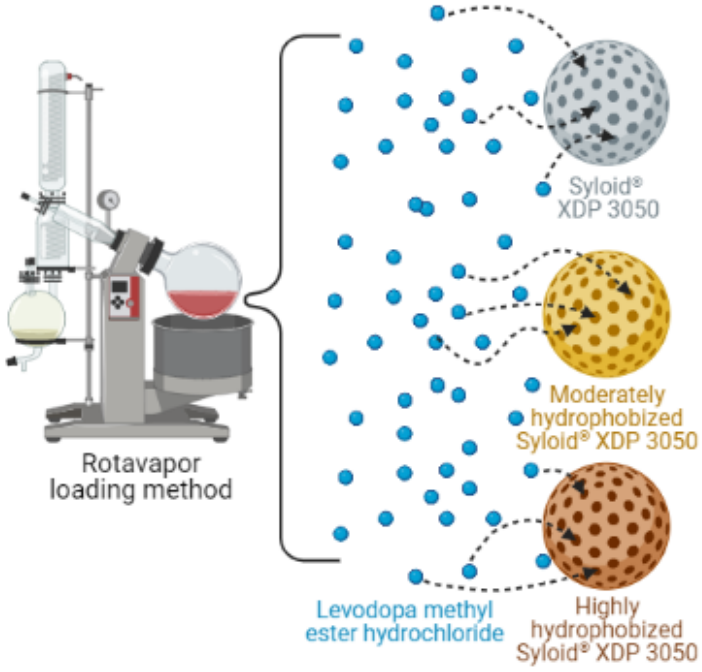

Figure 7. The loading process of LDME into MPS with the rotavapor method

The LDME and the given SYL were mixed and homogenized in a Turbula® blender mixer (Turbula System Schatz; Willy A. Bachofen AG Maschinenfabrik, Basel, Switzerland) using

60 rpm for 10 minutes to prepare physical mixtures. These powders were used as a reference in the measurements.

4.2.5. Particle size analysis with laser diffraction

The mean particle size of the co-ground products was characterized by the D_{50} value which was determined by a Malvern laser diffractometer (Malvern Mastersizer Scirocco 2000; Malvern Instruments Ltd., Worcestershire, UK). Air was used as the dispersion medium for the ground products from the entrance to the sample cell. During the measurements, the vibration feed rate was adjusted to 70 % and the dispersive air pressure was 3 bar. The refractive index of LD was 1.52.

4.2.6. X-ray powder diffractometry (XRPD)

The X-ray diffractograms were recorded with a Bruker D8 Advance diffractometer (Bruker AXS GmbH, Karlsruhe, Germany) with Cu K_α (λ= 1.5406 Å) and VANTEC-1 detector. The samples were scanned at 40 kV voltage and 40 mA amperage. The angular range was between 3-40 or 5-40 ° (2θ) and the increment was 0.007 °, the step time was 0.1 s. The samples were placed in a quartz holder at ambient temperature and relative humidity. The $K_{\alpha 2}$ radiation was stripped from the diffractogram, background correction, smoothening and evaluation were performed with DIFFRACTPLUS EVA software. Overall, the success of loading, the physical stability and the amorphization degree were determined by XRPD.

4.2.7. Scanning electron microscopy (SEM)

The morphology was of the products evaluated by a Hitachi S4700 scanning electron microscope (Hitachi Scientific Ltd., Tokyo, Japan) applying 10 kV acceleration voltage and 10 μA amperage. The samples were coated (90 s) with gold-palladium in a high vacuum evaporator by sputter coater.

4.2.8. Fourier transform infrared spectroscopy (FT-IR)

The mid-IR spectra of the samples (homogenized in 0.15 g KBr disks) were recorded in the spectral range of 400-4000 cm^{-1} with an AVATAR 330 FT-IR spectrometer (Thermo Nicolet, Unicam Hungary Ltd., Budapest, Hungary), equipped with a deuterated triglycine sulfate detector. The spectral resolution was 2 cm^{-1} and 128 scans were performed. OriginPro 8.6 software (OriginLab Corporation, Northampton, USA) was used for the spectral analysis. During sample preparation, the pressure was 10 tons and the diameter of the pressings was 13

mm; a Specac® Hydraulic Press was used. It was used for the evaluation of hydrophobization reaction and the secondary interactions between the API and the excipient.

4.2.9. Contact angle measurements

The apparent contact angle of the MPSs (Θ) was measured with an OCA 20 Optical Contact Angle Measuring System (Dataphysics, Filderstadt, Germany). The powder was compressed under a pressure of 3 tons by a Specac® hydraulic press (Specac Inc., USA). The contact angle of the pastilles was determined by using bi-distilled water test liquid. The measurements were performed at 25 °C. The volume of water droplets was 4.3 μl.

4.2.10. Streaming potential measurement-assisted particle charge titrations

The surface density of silanol groups of the SYLs was determined with streaming potential measurements assisted particle charge titrations. The streaming potential values in the 1 % w/V dispersions of the initial and the hydrophobized silica particles were measured with a PCD-02 Particle Charge Detector (Mütek Analytic GmbH, Germany). The negative surface charge excess of the silica particles was neutralized by 1 % w/V hexadecyl(trimethyl)ammonium bromide (CTAB) solution during particle charge titrations. The pH of the silica dispersions was adjusted to 11.3 with the help of NH_3/NH_4Cl buffer solution to ensure the complete deprotonation of the silanol groups (highly above the point of zero charge of silica) [113].

The charge-neutral states were achieved at streaming potentials of 0 mV. The specific surface charge excess values and therefore the specific silanol group densities were calculated according to the following equation assuming that the positive charge of a CTAB molecule neutralizes the negative charge of a deprotonated silanol group and the adsorption of NH_4^+ from the buffer on the silica surface is negligible:

$$d_{Si-OH} = \frac{V_{CTAB} \times c_{CTAB} \times N_A}{c_{SYL} \times V_{SYL} \times M_{CTAB} \times A_s \times 10^{18}}$$

where d_{Si-OH} is the surface density of the silanol group (1/nm^2), V_{CTAB} and c_{CTAB} are the volume (ml) and the concentration (g/100 ml) of the charge-neutralizing agent solution, respectively, N_A is the Avogadro constant (6.022*10^{23} 1/mol), V_{SYL} and c_{SYL} are the volume (ml) and the concentration (g/100 ml) of the silica dispersion, respectively, M_{CTAB} is the molar mass (364.45 g/mol) of the titrant CTAB, while A_s (m^2/g) is the specific surface of the silica. The initially

negative surface charge was reversed for each sample by adding an excess amount of titrant to the initial dispersion.

4.2.11. BET measurements

Nitrogen adsorption isotherms were recorded at 77 K using a QuantaChrome Nova 3000 surface area analyzer. Before the measurement, the samples were outgassed at 403 K for 1 h to remove any adsorbed contaminants. The specific surface areas (A_s) were calculated using the multipoint BET method based on six data points of the adsorption isotherms near monolayer coverage.

4.2.12. Differential scanning calorimetry (DSC)

3-5 mg samples were measured with Mettler-Toledo DSC-821e equipment (Greifensee, Switzerland). The samples were placed in a sample holder made from aluminium. The products were investigated in the temperature range of 25-350 °C with a heating rate of 10 °C/min. Each sample was normalized to the sample mass. The DSC curves were evaluated with STAR^e software.

4.2.13. The analysis of residual methanol content with gas chromatography (GC)

The methanol content of the samples was determined with the help of a gas chromatograph (Shimadzu GC-14B) equipped with thermal conductivity and a flame ionization detector. The calibration curve was previously determined in the range of 0 – 0.63 g/ml of methanol in ethanol medium. The concentration of methanol was directly proportional to the area of the peak for methanol.

4.2.14. Raman mapping to investigate the distribution of the API in the products

The distribution of LDME in SYLs was measured by Raman chemical mapping using a Thermo Fisher DXR Dispersive Raman instrument (Thermo Fisher Scientific Inc., Waltham, MA, USA), equipped with a CCD camera and a diode laser, operating at a wavelength of 780 nm. Raman measurements were carried out with a laser power of 24 mW at a slit aperture size of 50 μm. A surface with a size of 100 μm * 100 μm was analyzed with a step size of 10 μm, with an exposure time of 2 s and an acquisition time of 2 s, for a total of 6 scans per spectrum in the spectral range of 3500-200 cm^{-1} with cosmic-ray and fluorescence corrections. The Raman spectra were normalized to eliminate the intensity deviation between the measured areas.

4.2.15. *In vitro* release studies

- The release studies of nasal powders were performed in conditions corresponding to the nasal environment (30-32 °C, pH=5.60) while it was kept stirring. The volume of the dissolution

medium was adjusted to 50 ml and 5 ml of samples at predetermined times (5, 10, 15, 30 min) and filtered immediately (syringe filter: Minisart SRP 25, Sartorius, Göttingen, Germany; pore size: 0.2 μm) and the amount of dissolved drug was determined spectrophotometrically (PerkinElmer, Lambda 20 spectrophotometer, Dreieich, Germany). After sampling, it was replaced with 5 ml fresh dissolution medium. Taking the dilution into consideration, the dissolution profile and kinetics of each binary mixture were determined.

- In the case of the SYL-containing samples, the dissolution tests of the API were performed in a Hanson SR8 Plus release device (Hanson Research, CA, USA) in 100 ml of pH=6.8 phosphate buffer at 37 °C corresponding to the environment in the intestines. The stirring rate of the simple paddle was set at 100 rpm. 3 ml of samples were taken at predetermined time intervals (at 5, 10, 15, 30, 60, 90, 120, 180, 240, 300 min) and the volume was replaced with 3 ml of fresh dissolution medium. Prior to the measurements, 90 mg of the binary system (containing SYL loaded with LDME) was filled into a hard gelatine capsule (capsula operculata 00, Molar Chemicals, Budapest, Hungary). The capsule was placed in a seamless cellulose dialysis tubing (length: 8 cm, average flat width: 23 mm, Merck Ltd, Darmstadt, Germany).

The release kinetics from the products was determined. The fitting of the results was tested with zero order, first order, Higuchi, Korsmeyer-Peppas model and Hixson-Crowell cube root law [114]. The model for the fitting with the largest R^2 was accepted as the release kinetics.

- Dissolution can also be described by a saturation curve; thus the following equation can be used [115]:

$$\frac{m_{API,released}}{m_{API\ content}} = \frac{a * t}{1 + b * t}$$

where time is *t* (min) and we look for *parameters a* (1/min) and *b* (1/min), with which the equation the most closely fits the measured points. *Parameters a* and *b* were determined by iteration using the least-squares method (Solver extension of Excel 2016, Redmond, Washington, USA). This equation was proposed for so-called "lumped" second-order kinetics but we planned to investigate its utility for different release kinetics. It is advantageous to use this equation because it is model-independent and when the release is not complete, the application of this model does not distort the results.

If the limit of the equation is $t \rightarrow 0$:

$$\lim_{t\to 0}\frac{a*t}{1+b*t}=a*t=\frac{m_{API,initially\ released}}{m_{API\ content}}$$

Thus, *parameter a* corresponds to the initial release rate (IRR).

Thereafter, the difference (f_1) and the similarity factor (f_2) between the fitted model and the actual release results were calculated [116,117]. The difference factor (f_1) defines the percentage difference between two curves using the relative error between them:

$$f_1=\left\{\frac{\sum_{n=1}^{t}|R_t-T_t|}{\sum_{n=1}^{t}R_t}\right\}*100$$

The f_2 is the logarithmic reciprocal square root transformation of the sum of squared error and is a measurement of the similarity in the percent (%) dissolution between the two curves, i.e. it can be defined in the following way:

$$f_2=50*lg\left\{\left[1+\frac{1}{n}\sum_{t=1}^{n}(R_t-T_t)^2\right]^{-0.5}*100\right\}$$

In the defining equation of f_1 and f_2, the n is the number of observations, R_t is the mean percentage of drug dissolved from the reference formulation (in our case: the percentage of the model curve), T_t is the percentage of drug dissolved from the test formulation. As the value of f_2 approaches 100, the two compared curves are getting more and more similar. The similarity factor is considered a more appropriate method to compare release profiles [118].

4.2.16. High performance liquid chromatography (HPLC) methods

- *The quantification of LD-content:* LD-content was determined with an 1100 HPLC Agilent Series (Agilent Technologies, San Diego, CA, USA). An isocratic method was used with a C18 column (LiChroCART® 250-4 LiChrospher® 100 Å, pore size 5 µm) produced by Merck Millipore® (Merck Ltd., Darmstadt, Germany). The eluent was a mixture of phosphate buffer (pH=2.4):methanol=50:50 (v/v), the flow rate was adjusted at 0.5 ml/min, the injection was 20 µl and the analysis time was 10 min. The LD was analyzed at 280 nm with a diode array detector. Data were evaluated with ChemStation B.04.03. software (Agilent Technologies, Santa Clara, CA, USA).

- *The quantification of LDME-content:* as LDME is chemically unstable in aqueous media and is converted into LD during the release studies [67], it was necessary to follow the release

kinetics with HPLC to quantify both LDME and LD, the released amount of LDME was defined according to the next equation:

$$n_{LDME,released} = n_{LDME,measured} + n_{LD,measured}$$

where $n_{LDME,\ released}$ means the released moles of LDME, $n_{LDME,\ measured}$ and $n_{LD,\ measured}$ are the measured moles of LDME and LD, respectively.

The LDME-content was quantified with a 1260 HPLC Agilent system (Agilent Technologies, San Diego, CA, USA) equipment. The mobile phase consisted of acetate buffer (pH=5.0):methanol=90:10 (v/v). A Chrome-Clone™ 5 µm C18 100 Å column (150 x 4.6 mm, Phenomenex, Torrance, CA, USA) connected with a C18 security guard cartridge was applied. 10 µl of the sample was injected and isocratic elution was applied with 1.0 ml/min flow for 8 min at 30 °C. Both APIs were analyzed at 280 nm with a diode array detector. Data were evaluated with ChemStation B.04.03. software (Agilent Technologies, Santa Clara, CA, USA).

4.2.17. Stability tests

The stability of the LDME-containing powders was investigated under different conditions because of the expected instability of the API above 0 °C. They were investigated at -20 °C and 40 °C and relative humidity of 75 % (accelerated stability test) in a KKS TOP+ climate chamber (POL-EKO-APARATURA, Wodzisław Śląski, Poland) for 3 months, based on the ICH Q1A (R2) guideline proposal [119]. The accelerated stability tests were performed with the LD-containing nasal powders, as well.

During the chemical stability measurements, three parallels were measured.

4.2.18. Statistical evaluation of the results

The contact angle of the SYLs and the stability tests were evaluated by a 2-sample *t*-test with Minitab 17 Statistical Software (Minitab Ltd, UK). Besides, the statistical comparison of the *in vitro* release results of unique products was carried out by using the Tukey HSD test (n=3). A certain phenomenon was considered significant in the case of $p < 0.05$.

To investigate the quadratic response surface and to construct a polynomial model based on the *parameter a* values of the release results, TIBCO Statistica® 13.4 (Statsoft Hungary, Budapest, Hungary) statistical software was used. The significance of the variables and interactions based on their holistic effect was evaluated using analysis of variance (ANOVA). Differences were considered significant when $p < 0.05$.

5. RESULTS AND DISCUSSION

5.1. Preparation of LD-containing nasal powders

In this part of the work, we aimed to prepare nasal powders which can be proper to complementarily treat the *delayed on* periods of PD which belongs to one of the pharmacokinetics-related side effects of oral LD.

5.1.1. Construction of experimental design with the help of the QbD approach

As the LD-containing nasal powders are potentially able to reduce the *off* periods of PD during the LD treatment, therefore the knowledge space development aimed to map the potential risks and factors influencing the performance of the nasal powders. As part of the procedure, the QTPP was defined in the first step (Figure 8.). The QTPP comprised:

- administration route (intranasal);
- dosage form (nasal powder consisting of micronized or nano-in-micro particles);
- therapeutic indication (to reach systemic effect with low onset);
- physical stability;
- size of the product;
- drug release.

Thereafter, the following CQAs were chosen:

- wettability of the product;
- API crystallinity;
- immediate drug release;
- solubility;
- API particle size;
- stability.

In the next step, the directly controllable CPP/CMAs were defined which were:

- API-additive ratio;
- API initial particle size;
- rotational/milling speed;
- milling time.

A)

CQA \ QTPP	Administration route	Dosage form	Systemic effect	Physical stability	Size of the product	Drug release
Stability	Low	Medium	Low	High	Medium	High
Wettability (gel forming)	Low	High	Medium	Low	Medium	High
API crystallinity	Low	Low	Medium	High	High	Medium
Drug release (immediate)	Medium	Medium	High	Medium	High	Medium
Solubility	Low	Low	Low	Low	High	High
API particle size (in the formulation)	High	Low	High	Medium	High	High

B)

Process: Co-milling; CQA \ CPP/CMA	Rotational speed	Milling time	API-additive ratio	API initial particle size
Stability	Low	Low	Medium	Low
Wettability (gel forming)	Low	Low	High	Medium
API crystallinity	High	High	High	High
Drug release (immediate)	Medium	Medium	High	High
Solubility	Medium	Medium	Low	High
API particle size (in the formulation)	High	High	High	Medium

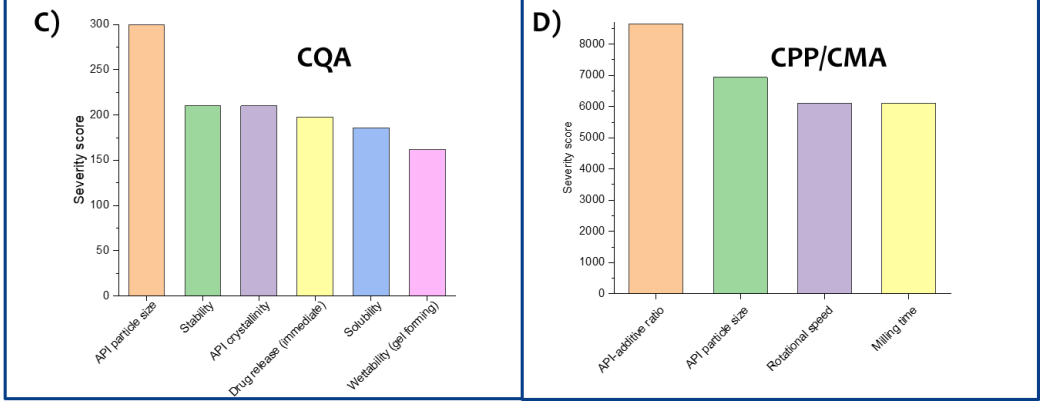

Figure 8. The results of the interdependence rating between the QTPP-CQA (A), the CQA-CPP/CMAs (B), the Pareto charts on the basis of the severity score of CQAs (C) and the CPPs/CMAs (D) using QbD-based RA to prepare LD-containing nasal powder with immediate release

Based on literature findings and previous experience, the RA showed that the mean particle size, the chemical stability, the API crystallinity and the release rate were mainly taken into consideration to characterize the products because these CQAs have the highest impact on the QTPP of the products when evaluating the properties of the formulations (Figure 8./C). Besides, the API-additive ratio (CPP) seemed to be the most significant factor in the performance of the products (Figure 8./D). The initial particle size distribution of API was standardized using a commercially available LD as starting material. The milling time and rotational speed were expected to have a similar effect on the properties. In the first step of the work, a pre-experiment was carried out to collect information about the preparation of binary nasal powders by co-milling: the LD:additive mass ratio, the rotational speed and the milling time were

systematically varied using two mucoadhesive excipients (CH and NaHA) as presented in Table 5.

In the next part, other binary nasal powders were formulated with five other excipients (α-CD, HPMC, PVP, PVA, MAN) which had been used for nasal drug delivery as well-known excipients with advantageous effects on this administration route. The LD:additive ratio and the milling time were varied, meanwhile, the rotational speed was fixed at 400 rpm based on the experimental results with CH and NaHA.

5.1.2. Physicochemical properties of the co-milled nasal products

The primary optimization of the products was executed on the basis of D_{50} values and crystallinity. As a result of co-milling, in general, the mean particle size of the powder mixtures drastically decreased and the API became partially amorphous, however, the excipients influenced the crystallinity of LD with different efficiency. A high extent of amorphization was measured in the case of CH and NaHA, lower crystallinity extent was detected when the ratio of the polymer was high (50:50 mass ratio). When the binary mixtures were co-milled with 400 rpm rotational speed, the crystallinity index of CH- and NaHA-containing powders was higher at 90 min in comparison to 60 min, which indicated partial recrystallization in this time interval. Besides, 400 rpm rotational speed was preferred over 300 rpm because a higher amorphization degree could be achieved. For these reasons, the 400 rpm rate was fixed and the milling lasted for a maximum of 60 min in the case of other formulations (containing α-CD, HPMC, PVP, PVA, MAN). The milling time and the LD:excipient ratio were varied during the optimization process. PVA hardly reduced the crystallinity because of the high initial particle size of the polymer resulting in a smaller extent of friction between the particles of the excipient and the API. Besides, the D_{50} value remained more than 40 μm, therefore it did not satisfy the pre-established requirements of nasal powders. The other binary powders were in the expected range. The physical properties of the optimized products are collected in Table 7.

Table 7. The co-milling parameters of the optimized products, the D_{50} value of the products and the given excipient as well as the detected secondary interactions

LD:additive	$D_{50,\ additive,\ initial}$ (µm)	Optimized mass ratio	Milling time (min)	Rotational speed (rpm)	$D_{50,\ formulation}$ (µm)	Detected secondary interaction
LD:CH	170.8	50:50	60	400	21.67	NO
LD:NaHA	166.3	50:50	60	400	13.07	NO
LD:α-CD	34.5	70:30	15	400	6.71	NO
LD:HPMC	221.2	70:30	60	400	13.72	NO
LD:PVP	66.1	50:50	30	400	7.67	YES
LD:PVA	2092.3	50:50	45	400	67.02	NO
LD:MAN	104.5	50:50	60	400	8.90	YES

The SEM images also verified the results of laser diffraction regarding the scale of mean particle size of the products (Figure 9.). The partially amorphous structure of the products can also be observed in the pictures based on the partially pounded instead of the sharp crystals.

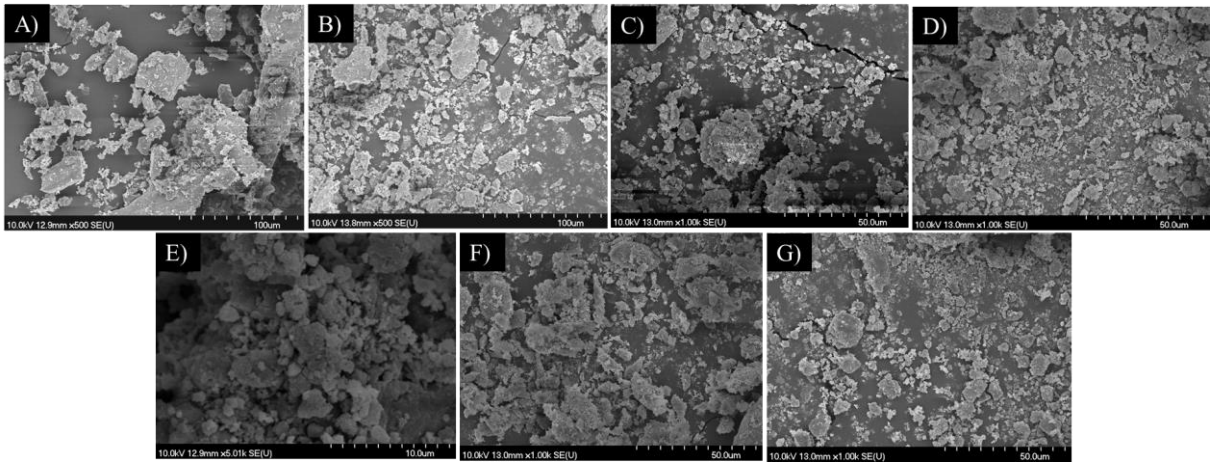

Figure 9. The SEM pictures of the LD:CH=50:50 (A), the LD:NaHA=50:50 (B), the LD:α-CD=70:30 (C), the LD:HPMC=70:30 (D), the LD:PVP=50:50 (E), the LD:PVA=50:50 (F) and the LD:MAN=50:50 (G) products

5.1.3. Secondary interactions between the LD and the excipients

The secondary interactions were evaluated by the comparison of a model spectrum (created from the linear combination of LD and the additive spectrum) to the product spectrum. T

$$x * [LD\ spectrum] + y * [additive\ spectrum] = [Model\ spectrum]$$

The *x* and *y* coefficients were varied by an iteration method with the help of the Solver extension of the Excel 2016 Software. The calculation minimized the *([Product spectrum] - [Model*

spectrum])^2 difference (*method of least squares*). To the best of our knowledge, it was the first time to use the method of least squares for the investigation of secondary interactions between an API and an excipient in solid-state with mid-IR spectroscopy. Secondary interaction could be detected only in the case of two products (Table 7.): the LD:PVP=50:50 and LD:MAN=50:50 (Figure 10.).

In the case of LD:PVP=50:50, the peak at 3387 cm^{-1}, which corresponded to the phenolic hydroxyl group of LD [120], increased to 3406 cm^{-1} wavenumber in the product. Besides, the broadening of this band also occurred which refers to the expansion of the hydrogen bonding system. The shift of the OH-stretching band and the broadening could be the consequence of the adsorbed water content of the polymer. These water clusters could play a role in the formation of hydrogen bonds.

The stretching band of the hydroxyl group belonging to LD also became broader but it was less remarkable in the LD:MAN=50:50 product. However, a well-defined strongly shifted ($\Delta\nu$=69 cm^{-1}) peak appeared at 1725 cm^{-1} on the spectrum of the product which could be assigned to the C=O asymmetric stretching mode of carboxylate of LD [120] which could be caused by intermolecular interaction between it and OH-groups of MAN.

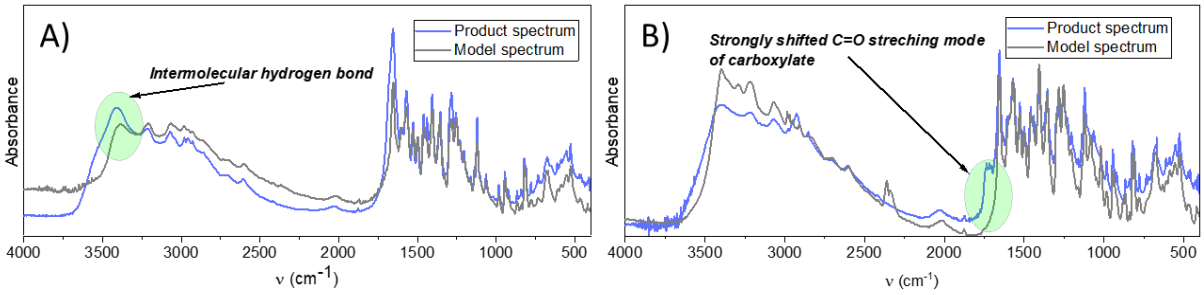

Figure 10. The model and the measured mid-IR spectrum of the LD:PVP=50:50 (A) and the LD:MAN=50:50 (B) products (the model spectrum was calculated from the linear combination of individual component spectra)

5.1.4. Short-term stability studies

After storage at 40 °C and relative humidity of 75 %, LD:CH=50:50, LD:PVA=50:50 and LD:PVP=50:50 samples showed a significant decrease in drug content after 2 months ($p < 0.05$), which could be due to the water-binding capacity of the polymers. LD may have been degraded by adsorbed water. No significant decrease ($p > 0.05$) was measured for the other samples and the reference raw LD powder, which can be considered stable over the 3-month

storage period. Based on these results, it can be concluded that LD is incompatible with CH, PVA and PVP because the chemical stability of the drug is reduced in the presence of these substances compared to the raw LD powder.

5.1.5. *In vitro* release from the LD-containing nasal powders

The *in vitro* drug release tests of binary mixtures were carried out by a modified dissolution method in artificial nasal media. Because of the limited residence time (a consequence of mucociliary clearance) on the nasal mucus and because the *delayed on* periods are aimed (emergency treatment), the API should own the quickest possible release rate. Thus, our purpose was to find the nasal powder whose dissolution rate was higher than the reference LD. According to our results, the LD:PVP=50:50, the LD:NaHA=50:50 and the LD:α-CD=70:30 were quicker than the reference (Figure 11.), the release of other products was slower during our experiments according to the $t_{15\ min}$ value. The *parameter a*, which characterized the IRR, gave the same sequence, except for the LD:PVA=50:50 which was quicker than the reference (Table 8.). Although, the PVP-containing formulation had the highest release rate, the LD:PVP=50:50 sample was not chemically stable, therefore it cannot be used as a nasal powder with LD. The model release curve constructed from the *parameters a* and *b* showed similarity with the actual release curve in each case.

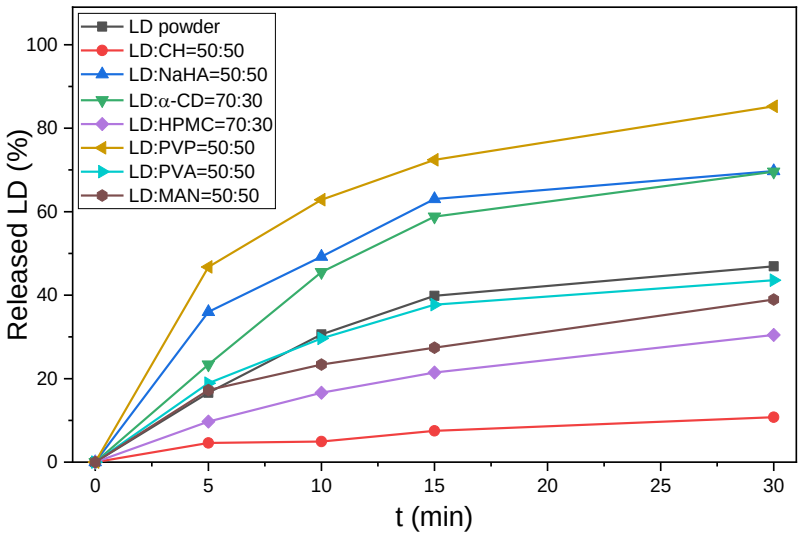

Figure 11. The release profile of the LD-containing products and the reference LD powder

Table 8. The parameters characterizing the release of the powders: the released ratio in 15 minutes of dissolution time ($t_{15\ min}$), the release kinetics, the *parameters a* and *b*, the difference and similarity factor between the model curve and the actual release curve

Products	$t_{15\ min}$ (%)	Release kinetics	*Parameter a* (1/min)	*Parameter b* (1/min)	f_1 (%)	f_2
LD powder	39.9	Hixson-Crowell	0.0531	0.0764	0.123	100.0
LD:CH=50:50	7.5	Could not be evaluated	0.00881	0.0501	8.23	100.0
LD:NaHA=50:50	63	Higuchi	0.1231	0.14	3.24	100.0
LD:α-CD=70:30	58.8	Hixson-Crowell	0.0763	0.0729	6.23	100.0
LD:HPMC=70:30	21.5	First-order	0.0241	0.0456	0.2756	100.0
LD:PVP=50:50	72.4	Hixson-Crowell	0.168	0.165	0.714	100.0
LD:PVA=50:50	37.7	Hixson-Crowell	0.0603	0.102	3.25	100.0
LD:MAN=50:50	27.4	Higuchi	0.0431	0.0804	5.04	100.0

The slow dissolution from the LD:MAN=50:50 sample could be due to the secondary interactions between the API and the additive. As LD basically has a relatively high dissolution rate, MAN could hinder the release of the API. The LD:HMPC=70:30 and the LD:CH=50:50 products could be used for extended drug delivery if the formulation could adhere to the nasal mucosa for a longer period of time because they form a highly viscous gel after the absorption of water. Thus, these excipients are not suggested to use in the nasal delivery of LD for the treatment of the *delayed on* periods.

5.1.6. Potential feasibility of the nasal powders based on the results

LD-containing nasal powders were optimized by co-milling to reach the formulation which can potentially be proper for the treatment of the *delayed on* periods of PD. The optimization was carried out to prepare a formulation that satisfied the requirements regarding the D_{50} value (more than 5 μm to prevent it from reaching the lungs but less than 45 μm to exhibit fast release), in which the LD is chemically stable and whose release rate is higher than the reference. Based on our findings, the LD:NaHA=50:50 and the LD:α-CD=70:30 nasal powders could be used as

a complementary treatment to the conventional oral LD administration. The LD:PVP=50:50 also exhibited a quick release rate but it was not chemically stable. The release rate of LD:PVA=50:50 was similar to the LD reference but its D_{50} value was higher than 45 μm. The NaHA and the α-CD could be also mixed in the future to prepare a ternary nasal powder with increased mucoadhesion and absorption rate potentially resulting in improved bioavailability.

5.2. The preparation of LDME-containing hydrophobized silica for oral administration

In this part of the Ph.D. work, we intended to formulate and optimize MPS microparticles loaded with LDME to reach extended drug release and zero-order kinetics to suggest a potentially suitable, stable formulation that might lead to reduced *wearing off* periods of PD compared to the conventional oral administration of LD-containing tablets.

5.2.1. RA and construction of experimental design with the help of the QbD approach

The LDME-containing MPS powders were planned for oral administration for patients with advanced PD, therefore the QTPP was the following:

- efficiency (therapeutical efficiency);
- steady blood level (advanced PD);
- indication (extended drug release);
- administration route (oral);
- targeted patient population (patients with advanced PD);
- dosage form (powder for capsule filling).

As the dissolution of LDME is required to be prolonged, therefore the wetting properties of the formulation are crucial to know and control. Besides, too much amount of a drug might lead to precipitation on the surface of MPS resulting in inhomogeneity, therefore it is important to test the dependence of the physical stability on the drug ratio. We also have to take into account that the LDME is chemically unstable at room temperature. Based on the above-mentioned reasons, the following CQAs were chosen:

- physical stability;
- chemical stability;
- extended release;
- homogeneity of the API;
- wetting properties.

In the following step, the CPPs and the CMAs were taken into account, two steps of the formulation process were identified:

1) SYL hydrophobization:

- the water content of the system;
- TMCS concentration;
- reaction time;
- reaction temperature;
- relative humidity.

2) SYL loading:

- applied temperature during the vacuum evaporation
- applied vacuum during the vacuum evaporation
- type of the solvent
- volume of the solvent
- pore volume of the silica
- LDME:SYL ratio.

The connection between the QTPP-CQA and the CQA-CPP/CMA is summarized in Figure 12.

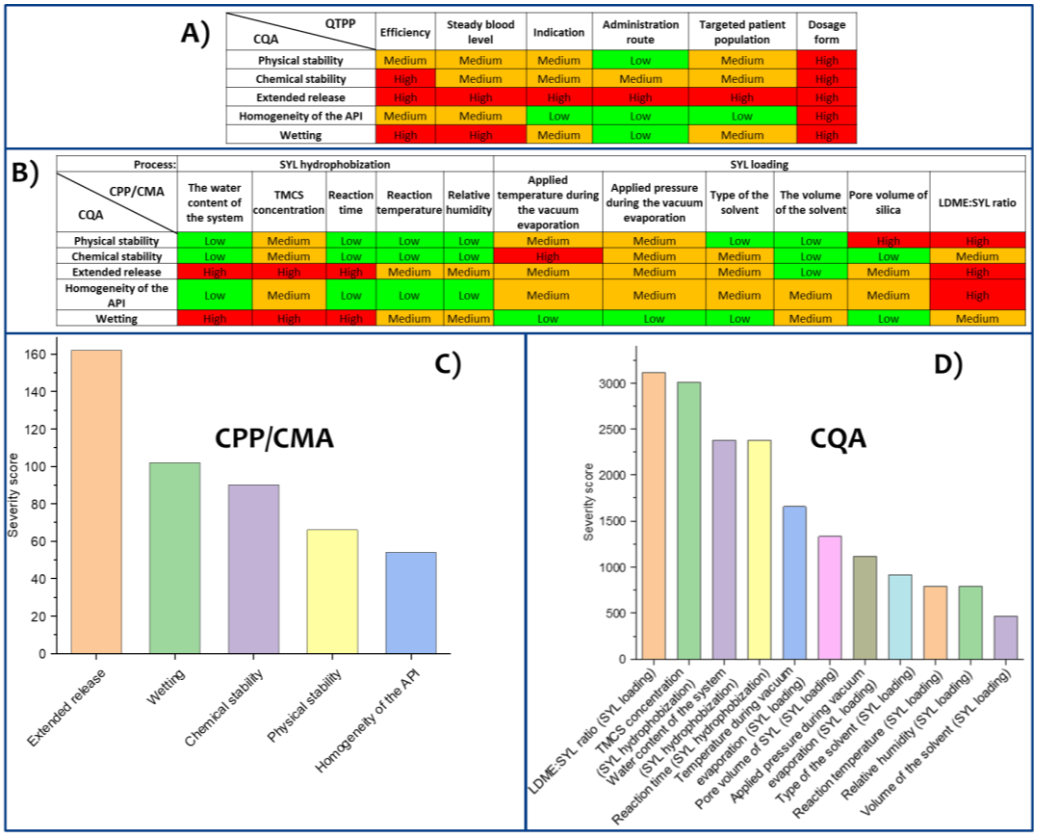

Figure 12. The results of the interdependence rating between the QTPP-CQAs (A), the CQAs-CPP/CMAs (B), the Pareto charts based on the severity score of CQAs (C), and the CPPs/CMAs (D) using QbD-based RA to prepare LDME-containing MPS microparticles with extended release

The initial RA showed that the extended release of the API from the formulations and the wetting properties were the most influencing factors on the QTPP among the CQAs. The CQAs can be controlled mainly by varying the LDME:SYL ratio during the SYL loading and by varying the hydrophobization agent concentration during the SYL hydrophobization process Thus, a 3^2 full-factorial design was set, the factors are presented in Table 6.

5.2.2. The hydrophobization of the SYL-0 to control the drug release

Based on the preliminary experiments and the initial RA, the moisture content had a key role in the success of the reaction. It was revealed that in case the SYL-0 particles had been dried at 110 °C before the process, the chemical reaction did not undergo. For this reason, the adsorbed moisture content of the SYL-0 particles had been equilibrated for 3 days at 40 °C and relative humidity of 75 % prior to the reaction. Increasing the concentration of TMCS during the reaction showed an increasing tendency in the change of contact angle with water. According to the charge titration measurements, the surface density of the Si-OH groups decreased due to the functionalization by increasing the concentration of reactant (Table 9.).

Table 9. The contact angle and the surface density of silanol groups of initial SYL-0 and its hydrophobized derivatives (SYL-1 and SYL-2)

SYL	Θ_{H2O} (°)	$d_{Si\text{-}OH}$ (1/nm^2)
SYL-0	0	0.64
SYL-1	66.86 ± 7.16	0.54
SYL-2	120.49 ± 2.78	0.15

The decrease of silanol groups could be also a consequence of the high drying temperature (70 °C) after the reaction, therefore the presence of $–Si(CH_3)_3$ groups also needed to be verified. Remarkable differences in the mid-IR spectra of SYL-1 and SYL-2 were detected after the modification compared to the SYL-0 (Figure 13.).

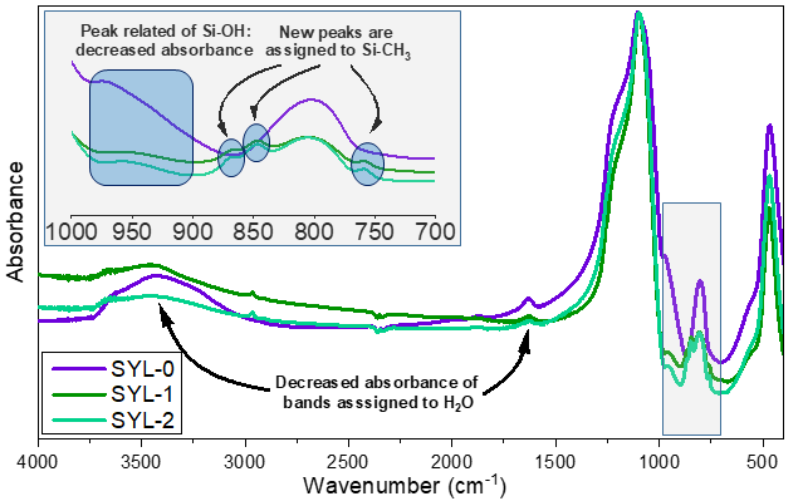

Figure 13. Mid-IR spectra of SYL-0, SYL-1 and SYL-2; the 700–1000 cm^{-1} region is magnified

The bands at 474, 804 and a shoulder type peak at 1105 cm^{-1} with a shoulder at 1188 cm^{-1} were assigned to the vibrations of siloxane (-Si-O-Si-) groups which were intact in the reaction [121]. The band at 972 cm^{-1} could be ordered to the stretching vibrations of the silanol (-Si-OH) groups, the intensity of this band decreased after hydrophobization indicating a significant reduction of the silanol group density. The spectral range of 865–750 cm^{-1} (peaks on the spectra at 759, 850 and 865 cm^{-1}) could be assigned to the presence of $–Si-CH_3$ [122] verifying the successful surface modification. Meanwhile, the bands at 1633 and 3435 cm^{-1} belonged to the vibrations of the adsorbed water molecules [121]. The intensity of these peaks decreased in the case of the hydrophobized silica, nevertheless, they were stored under the same conditions after the reaction. It indicated that fewer amount of water could be adsorbed on the surface of SYL-1 and SYL-2 than that of SYL-0 probably due to the lower hydrophilic surface silanol content. The hydrophobization caused reduced nitrogen adsorption capacity [123] which phenomenon had been experienced in the literature, therefore the BET specific surface of the SYLs was the following: SYL-0=283 m^2/g, that of the SYL-1=244 m^2/g and that of the SYL-2=235 m^2/g. Its reason could probably be that the new groups reduced the diameter of mesopores because the attached trimethylsilyl groups were larger than the silanol groups.

5.2.3. The loading of LDME into the SYL mesopores

Based on the detailed mechanisms described in the literature, if the API is successfully loaded into MPS, it will become amorphous, however, in the case of applying API in excess, it might

recrystallize on the outer surface of the carrier. Thus, XRPD and DSC measurements could indicate whether the loading process was successful. Applying LDME in 20 % w/w or lower amount, the API could be incorporated into the SYLs (Figure 14.), which was proven by the absence of crystalline peaks on the diffractogram and melting point on the DSC curve. In contrast to trials with 40 and 60 % w/w (SYL-0-40 and SYL-0-60 on the Figure 14./A, respectively) drug ratio, characteristic peaks appeared on the diffractograms in these cases but the 2θ values were different from peaks corresponding to the initial LDME (LDME-I).

Prior to the evaporation, the LDME and the SYL were dispersed in methanol, therefore formulation could contain residual methanol content whose amount is limited by the ICH Q3C (R8) guideline at 3000 ppm (w/w) [59]. According to the results of the GC, the amount of this organic solvent in each product was below the limit.

The specific surface area of the loaded SYLs decreased after loading drug loading. In addition, as the loading extent increased, the surface area decreased (Table 10.).

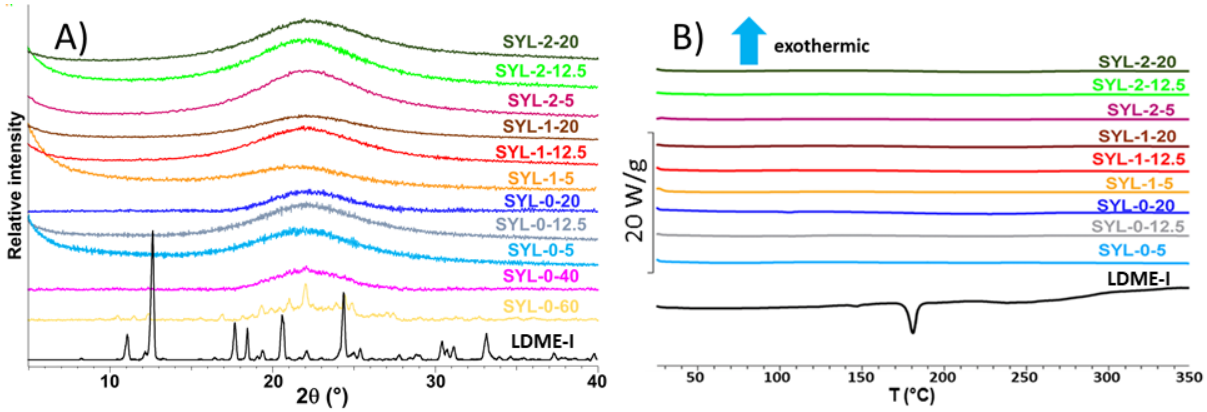

Figure 14. The diffractograms (A) and the DSC curves (B) of the formulations

5.2.4. Polymorph screening of LDME by crystallization

When 40 and 60 % w/w ratio of LDME was used, new characteristic peaks appeared on the diffractograms immediately after the loading process but they did not correspond to the peaks of initial LDME, which phenomenon could refer to the formation of a new polymorph of LDME on the SYL surface during the evaporation. Therefore a crystallization study was performed with LDME by evaporation of ethanol, methanol and purified water. Each solvent led to the same polymorph form (LDME-II) which was also detected in the case of the SYL loading trial with a high amount of API. According to the DSC, the LDME-II had a lower melting point (138 °C) than the initial LDME (LDME-I) (178 °C). Above the melting point of LDME-II, it

recrystallized into LDME-I. After heating the LDME-II between the melting point of LDME-II and LDME-I (to 145 °C), the XRPD pattern showed the characteristic peaks of LDME-I (Figure 15.), i.e. the LDME-II could convert back to LDME-I. These results presumably suggest that a new polymorph of LDME was identified.

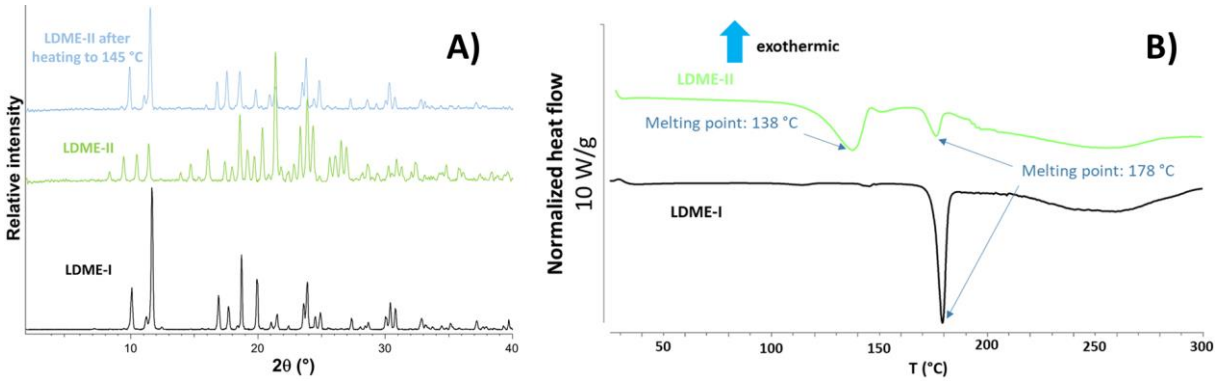

Figure 15. The diffractogram (A) and the DSC curve (B) of LDME-I and LDME-II, as well as the diffractogram of LDME-II after heating to 145 °C (A)

5.2.5. The distribution of LDME in the formulations

Raman mapping was performed to explore the distribution of LDME in the products (Figure 16.). The Raman spectrum of pure LDME was used as a reference to visualize the chemical map of the products showing the amount of LDME. The increasing amount of LDME during the loading process caused a larger extent of regions on the chemical map (red colour) and more intensive peaks on the Raman spectra due to the higher amount of API in the system. In the SYL 1-5 and SYL 2-5 products, the LDME can be found only sporadically in contrast to SYL 0-5, which can be attributed to the strong interactions between the polar API and the polar silanol and siloxane groups on the surface but the LDME-LDME interaction might become dominant over the LDME-SYL interactions in the hydrophobic products because of the decrease in the polar functional groups. Overall, in the range of 5-20 % w/w of LDME, a homogeneous distribution of the API was observed in the products which referred to the efficient incorporation process.

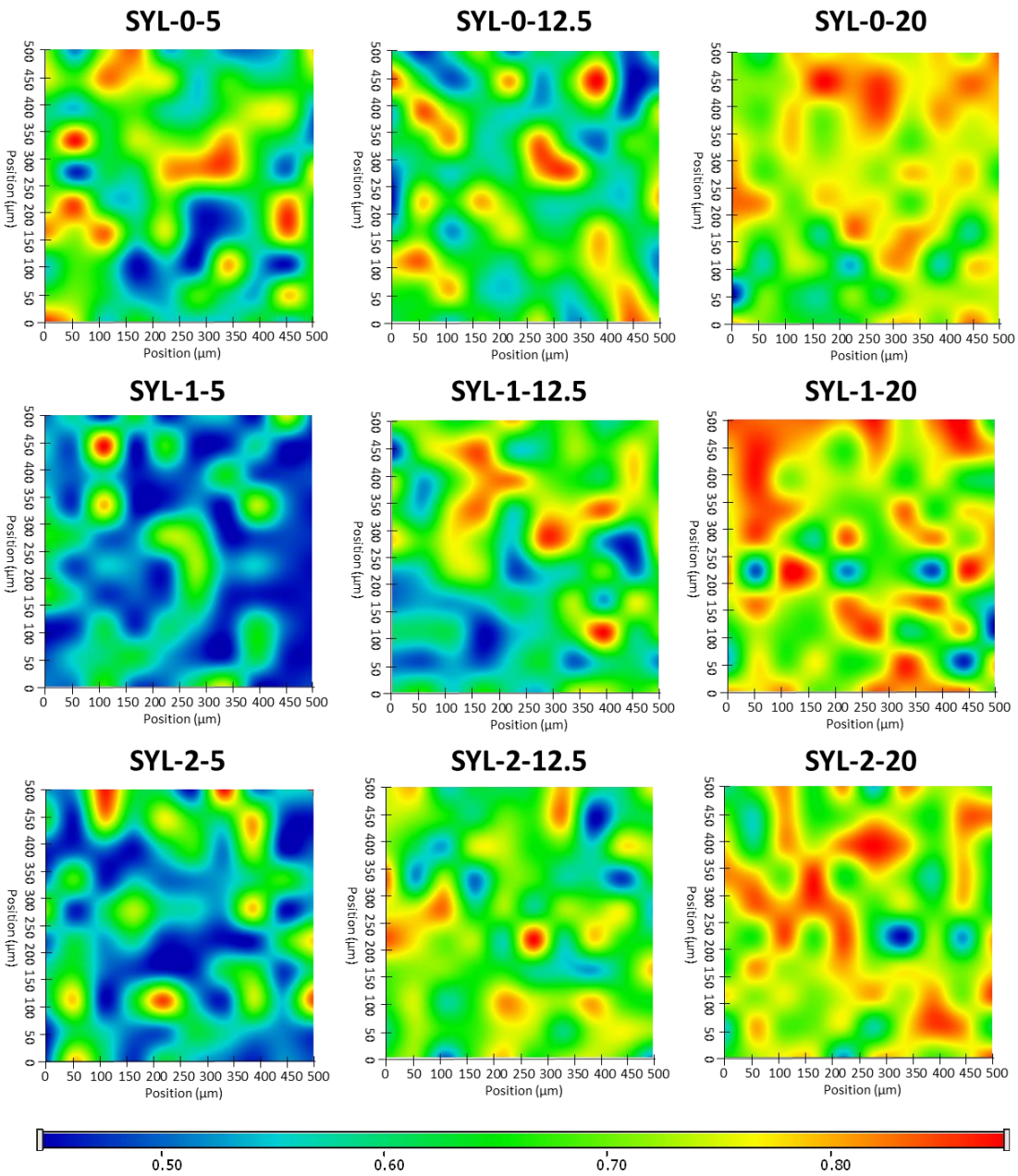

Figure 16. Raman chemical maps showing the distribution of LDME in the products

5.2.6. Short-term stability studies

The chemical stability of the SYL-LDME binary powders was appropriate upon storage in the freezer (-20 °C); however, the drug content decreased at 40 °C and relative humidity of 75 % indicating that the LDME-containing formulations should be stored in the freezer to preserve chemical stability. On the other hand, low-intensity peaks of the API appeared on the

diffractogram of SYL-0-20 after 3 months of storage at -20 °C, which indicated that 20 % w/w of API might be high enough to indicate recrystallization.

5.2.7. *In vitro* release from the LDME-containing SYL formulations

As a general tendency, the release rate of LDME could be distinguished according to the hydrophobicity of SYL. The release studies showed that the increased hydrophobicity of SYL decreased the drug release rate. The SYL-2-containing formulations with the same ratio of loaded LDME showed spectacularly slower drug release in comparison to SYL-0- and SYL-1-containing ones, however, the difference was smaller in the case of 20 % w/w LDME-containing formulations (Figure 17.). The difference between the SYL-2-containing and the other formulations could be explained by the poor aqueous wettability of SYL-2 compared to SYL-0 and SYL-1.

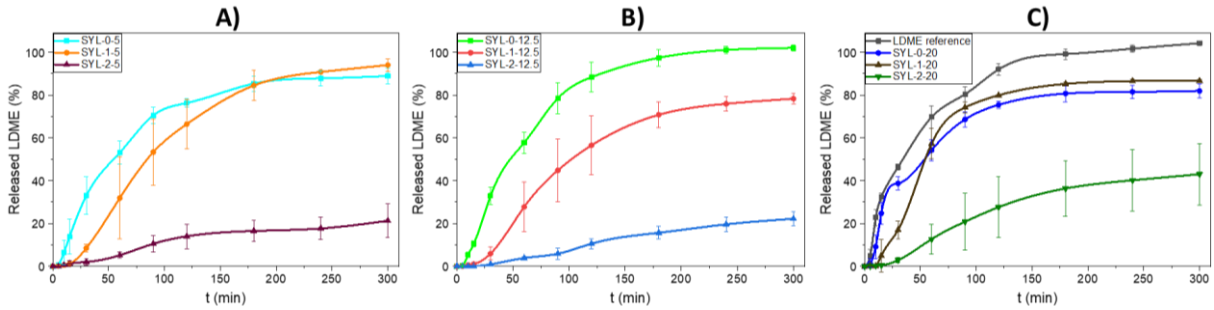

Figure 17. The *in vitro* release curves of the 5 % w/w (A), the 12.5 % w/w (B) and the 20 % w/w LDME-containing products as well as the reference LDME (C)

The kinetics of the drug release curves were determined. The first-order kinetics was observed in the case of reference LDME, SYL-0-20, SYL-1-20 and SYL-2-20 products presumably due to the relatively high loading extent. The dissolution of LDME from SYL-0-5, SYL-0-12.5, SYL-1-5 and SYL-1-12.5 products fitted to the Hixson-Crowell model with the strongest correlation probably because the surface area decreased as the drug released. The SYL-2-5 and SYL-2-12.5 exhibited zero-order release kinetics, which was one of the main purposes of our formulation development as they are expected to be able to provide a steady blood level. *Parameters a* and *b* were used to quantifiably interpret the results, the IRR was characterized with the help of *parameter a*. Using these parameters, a model release curve could be established, the similarity between the actual and model results could be established (Table 10.).

Table 10. The release parameters (*a* and *b*), the specific surface area, the release kinetics of the products and the reference LDME, the difference and the similarity factors between the model curve and the actual release results

Sample	***Parameter a* (1/min)**	***Parameter b* (1/min)**	**A_s (m^2/g)**	**Release kinetics with the strongest correlation**	**f_1 (%)**	**f_2**
LDME reference	0.02659	0.02165	-	First order	0.125	99.99
SYL-0-5	0.01600	0.01363	263	Hixson-Crowell	7.82	99.98
SYL-0-12.5	0.01585	0.01116	255	Hixson-Crowell	9.57	99.96
SYL-0-20	0.02006	0.01993	208	First order	6.73	99.98
SYL-1-5	0.007694	0.004263	240	Hixson-Crowell	13.8	99.95
SYL-1-12.5	0.0065001	0.004281	184	Hixson-Crowell	14.0	99.96
SYL-1-20	0.01371	0.01103	181	First order	17.3	99.91
SYL-2-5	0.001359	0.002931	226	Zero order	11.4	100.0
SYL-2-12.5	0.0008355	0.002598	173	Zero order	12.4	100.0
SYL-2-20	0.002804	0.002509	169	First order	12.0	99.99

A polynomial equation could be established to define the relationship between the dependent variable (*parameter a*) and the independent variables (c_{TMCS} and *% w/w of LDME*).

$$Parameter\ a = 9.423*10^{-3} \mathbf{- 7.818*10^{-3}\ x} - 9.1*10^{-5}\ x^2 \mathbf{+ 1.921*10^{-3}\ y - 1.271*10^{-3}\ y^2} - 6.55*10^{-4}\ x\ y + 2.33*10^{-4}\ x\ y^2 + 8.15*10^{-3}\ x^2\ y - 6.23*10^{-4}\ x^2\ y^2$$

where *x* corresponds to the TMCS concentration; *y* corresponds to the LDME mass percent when mixing the LDME with SYL. The members of the equation exhibiting a significant influence on *parameter a* were highlighted in bold. The statistical parameters of this equation were: $R^2 = 0.93462$, adjusted $R^2 = 0.90556$, mean square residual = $4.8*10^{-6}$. The removal of two members with the highest *p*-value ($-9.1*10^{-5}\ x^2$; $2.33*10^{-4}\ x\ y^2$) from the polynomial equation, resulted in the closest fit to the measured points resulting in the following equation:

$$Parameter\ a = 9.423*10^{-3} \mathbf{- 7.818*10^{-3}\ x + 1.921*10^{-3}\ y - 1.271*10^{-3}\ y^2} - 6.55*10^{-4}\ x\ y + 8.15*10^{-3}\ x^2\ y - 6.23 \times 10^{-4}\ x^2\ y^2$$

The statistical parameters of this equation were: $R^2 = 0.93381$, adjusted $R^2 = 0.91395$, mean square residual = $4.4*10^{-6}$. The members of the equation exhibiting significant influence on the *parameter a*, were highlighted in bold. This equation defined a surface plot (Figure 18.):

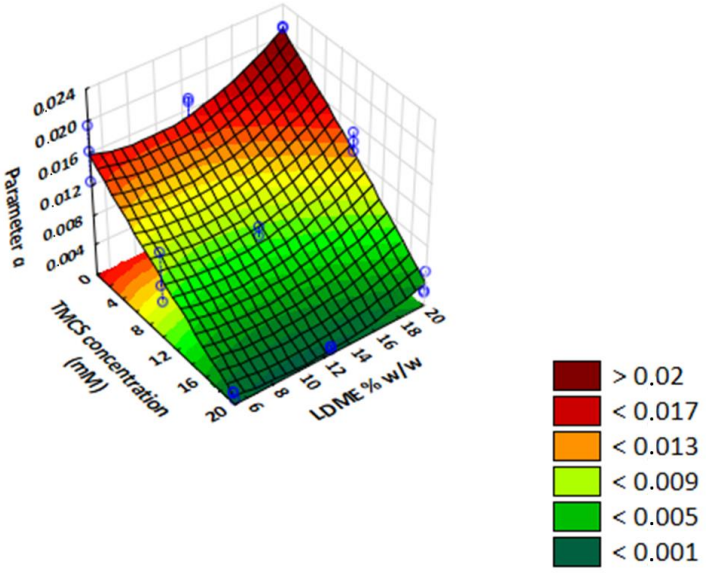

Figure 18. The surface plot of the *parameter a* as a function of TMCS concentration and LDME % w/w (the $-\ 9.1*10^{-5}\ x^2$ and the $2.33*10^{-4}\ x\ y^2$ members are ignored from the polynomial equation)

The results indicated that LDME % w/w had a positive significant effect and a negative quadratic effect on *parameter a*, meanwhile, the increase of the hydrophobization extent (as the TMCS concentration increased) significantly decreased the drug release rate. The results of Tukey HSD test showed that the release rate was significantly lower for each product than for the LDME reference, except for SYL-0-20 (Figure 19.). Based on the ANOVA evaluation of the results of the 3^2 full-factorial design, the LDME mass percent did not exhibit a significant effect on the *parameter a* when the individual values were compared. This the apparent contradiction between the ANOVA and the individual Tukey HSD tests emphasizes the importance of the holistic approach of ANOVA evaluation of factorial designs.

The results of Tukey the HSD test implied that the *parameter a* of SYL-2-containing products at a given LDME % w/w was significantly lower than SYL-0-containing ones, however, there was no significant difference between the SYL-0- and SYL-1-containing samples indicating that the use of 20 mM of hydrophobization agent was satisfactory to decelerate the drug dissolution rate in contrast to 10 mM. According to the results, the limiting factor of preparing drug-loaded MPS is the small amount of material that can be incorporated into the mesopores resulting in a system without even partially recrystallized API. Thus, the wetting properties and

the loading extent of the carrier must be taken into account in the case of the development of an MPS-based drug delivery system because they have a significant effect on the release kinetics and the stability.

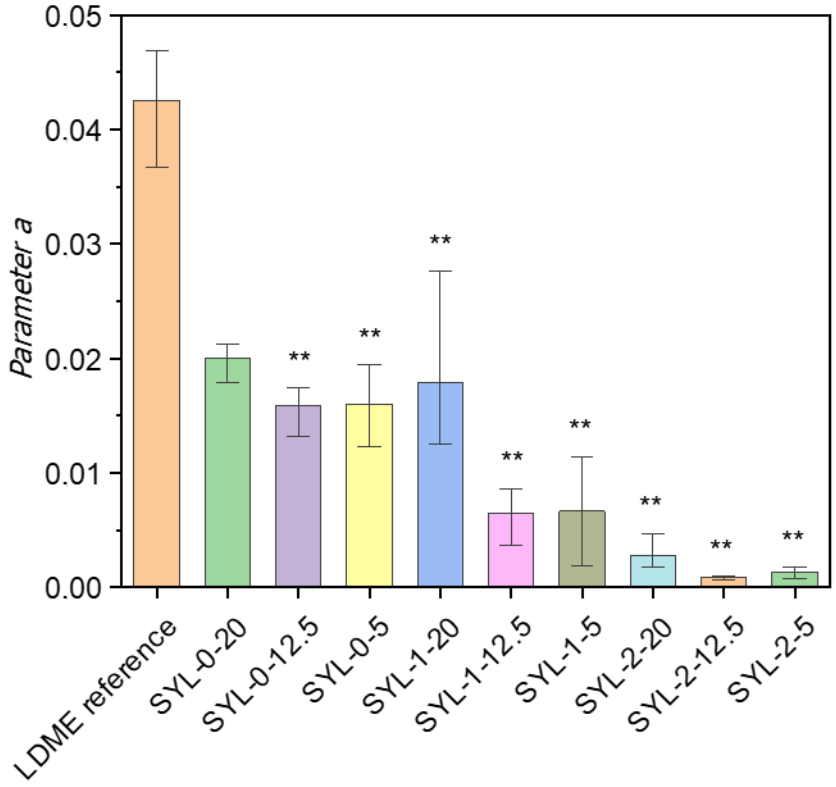

Figure 19. The *parameter a* of the LDME reference and the LDME-containing formulations, the significant difference between the product and the LDME is marked with asterisks

5.2.8. Potential feasibility of the LDME-containing SYL systems based on the results

During our work, surface-modified MPSs were synthesized via hydrophobization with TMCS, then antiparkinsonian LDME was loaded into the mesopores with the so-called rotavapor method. The hydrophobization was evaluated with streaming potential measurement-assisted particle charge titrations, contact angle measurements and FT-IR The successful loading was verified with XRPD, DSC, Raman mapping and BET.

The optimized formulations were stable and exhibited zero-order release kinetics and controlled release (SYL-2-12.5 and SYL-2-5) which can provide a steady blood level leading to decreased side effects. A similar approach is used in the LD/carbidopa-containing duodenal infusion [124].

The use of hydrophobized MPSs can be suggested for APIs with a narrow therapeutic index (like dopamine precursors when PD is advanced) because the API release can be systematically controlled via the wettability of MPSs and the API content.

5.3. The perspectives of possible utilization of the formulations

In this Ph.D. work, formulations containing dopamine precursors (LD, LDME) were prepared both for intranasal and oral delivery using the QbD approach. The nasal powders can exhibit a short offset after administration, therefore they can be suitable to treat the *delayed on* periods of PD. The most promising nasal powders were the LD:NaHA=50:50 and the LD:α-CD=70:30, the NaHA and the α-CD could also be combined to further optimize the properties.

Besides, LDME was loaded into the pores of non-hydrophobized and hydrophobized MPS to prepare formulations with zero-order release kinetics and extended release. These powders are suitable to fill into capsules and administered orally. The optimized formulations were SYL-2-12.5 and SYL-2-5 for the possible treatment of *wearing off* periods.

As a conclusion of the results, nasal powder and oral capsule were formulated and the drug release of LD and LDME was controlled. The results can provide additional information to the developers to prepare formulations that have an improved pharmacokinetic profile than the conventional oral immediate release tablets.

6. CONCLUSIONS

The novel results of this Ph.D. work aim to prepare innovative LD- and LDME-containing nasal and oral dosage forms, that is be summarized in the following points:

I) During this work, dopamine prodrug-containing powders were formulated. There are only a few studies in the literature dealing with the formulations of LD as nasal powder despite the advantages like higher stability in solid form, higher applicable doses, higher residence time on the nasal mucosa and quicker absorption rate. Besides, to the best of our knowledge, it had not been explored if the LDME release rate can be prolonged by loading into hydrophobized MPS.

II) Using the data of the detailed literature review and the pre-experiments of the research group on this field, we applied the QbD approach to define the QTPP, CQAs, CPP/CMAs. The most influencing factors were chosen to control and optimize the critical properties of the formulations by experimental designs.

III) LD-containing binary nasal powders were prepared by co-milling the LD and an excipient. The primary optimization of LD-containing nasal powders was carried out based on the mean particle size. There was at least one ratio of LD:excipient in the case of a given excipient which satisfied the requirements of mean particle size, except for the PVA-containing samples whose D_{50} value were always higher than 45 μm. The co-milling also resulted in amorphization for 60 min, however, recrystallization occurred in some products between 60-90 min. Secondary interactions were detected in the LD:PVP=50:50 and LD:MAN=50:50 between the components which could influence the *in vitro* release results. The chemical stability of the LD:CH=50:50, the LD:PVA=50:50 and the LD:PVP=50:50 powders was not satisfactory because there was a significant decrease in LD-content after 2 months of storage at 40 °C and relative humidity of 75 % referring to incompatibility between the components. However, the other formulations as well as the reference raw drug powder were chemically stable during the 3 months of storage. The *in vitro* drug release rate of the LD:PVP=50:50, the LD:NaHA=50:50 and the LD:α-CD=70:30 was quicker than the reference LD powder. The results showed that NaHA and α-CD were compatible with LD.

IV) The surface of MPS was hydrophobized with TMCS to reduce the wetting properties. The effect of surface modification on the change of silica properties was confirmed by contact angle measurements, streaming potential measurement-assisted particle charge titrations and FT-IR. Thereafter, the LDME was loaded into the mesopores with rotavapor method, meanwhile, the

LDME was dissolved in methanol. The hydrophobization and the loading extent was optimized to prepare formulations which might provide steady blood level of the API. The residual methanol content was below the limit defined by ICH Q3C (R8) guideline. The products were not chemically stable at 40 °C and relative humidity of 75 % but they were chemically stable during the storage in a freezer (-20 °C) for 3 months. The loading ratio of LDME was investigated to evaluate the maximum possible amount of API that can remain in the pores without recrystallization: a small number of crystalline peaks was detected on the diffractogram in the case of SYL-0-20 after 3 months of storage at -20 °C. When the LDME crystallized during the loading process, new peaks appeared on the diffractogram which did not correspond to the peaks of the initial LDME. For this reason, a detailed crystallization study was performed: the LDME was crystallized from water and some organic solvents including methanol. The diffractogram and the DSC curve of this crystal form were different from the commercially available one which probably referred to the formation of a new polymorph. As the SYL-2-5 and SYL-2-12.5 products had zero-order release kinetics and an extended release profile and they were stable at -20 °C, they can be considered the optimal formulations.

V) Based on the release profile and the physicochemical properties, the oral products exhibiting extended release (SYL-2-5 and SYL-2-12.5) can reduce the *wearing off* periods and the nasal powders with immediate release (LD:NaHA=50:50 and LD:α-CD=50:50) can be proper for the treatment of *delayed on* periods.

The main new findings and practical aspects of the work:

✓ Determination of factors influencing the expected performance of LD-containing nasal powders and oral hydrophobized MPSs loaded with LDME using the QbD approach.

✓ LD-containing nasal powders for the treatment of *delayed on* periods of PD were formulated and optimized. The interaction studies revealed that LD was compatible with α-CD and NaHA and incompatible with other excipients.

✓ LDME was loaded into the pore system of a hydrophobized MPS for the very first time. The extent of hydrophobization and the loading ratio were optimized to prepare a stable formulation that exhibited extended release and zero-order release kinetics to treat the *wearing off* periods.

✓ A new polymorph of LDME (LDME-II) was presumably discovered and its physicochemical properties were compared to the initial LDME (LDME-I) which is crucial from industrial aspect.

REFERENCES

1. Müller, T. Pharmacokinetics and Pharmacodynamics of Levodopa/Carbidopa Cotherapies for Parkinson's Disease. **2020**, *16*, 403–414, doi:10.1080/17425255.2020.1750596.
2. Zangaglia, R.; Stocchi, F.; Sciarretta, M.; Antonini, A.; Mancini, F.; Guidi, M.; Martignoni, E.; Pacchetti, C. Clinical Experiences with Levodopa Methylester (Melevodopa) in Patients with Parkinson Disease Experiencing Motor Fluctuations: An Open-Label Observational Study. *Clin. Neuropharmacol.* **2010**, *33*, 61–66, doi:10.1097/WNF.0B013E3181C5E60C.
3. Antonini, A.; Odin, P.; Pahwa, R.; Aldred, J.; Alobaidi, A.; Jalundhwala, Y.J.; Kukreja, P.; Bergmann, L.; Inguva, S.; Bao, Y.; et al. The Long-Term Impact of Levodopa/Carbidopa Intestinal Gel on 'Off'-Time in Patients with Advanced Parkinson's Disease: A Systematic Review. *Adv. Ther.* **2021**, *38*, 2854–2890, doi:10.1007/S12325-021-01747-1/TABLES/7.
4. Lipp, M.M.; Hickey, A.J.; Langer, R.; LeWitt, P.A. A Technology Evaluation of CVT-301 (Inbrija): An Inhalable Therapy for Treatment of Parkinson's Disease. **2021**, *18*, 1559–1569, doi:10.1080/17425247.2021.1960820.
5. Jankovic, J. Motor Fluctuations and Dyskinesias in Parkinson's Disease: Clinical Manifestations. *Mov. Disord.* **2005**, *20*, S11–S16, doi:10.1002/MDS.20458.
6. Huang, Z.; Kunnath, K.T.; Han, X.; Deng, X.; Chen, L.; Davé, R.N. Ultra-Fine Dispersible Powders Coated with l-Leucine via Two-Step Co-Milling. *Adv. Powder Technol.* **2018**, *29*, 2957–2965, doi:10.1016/J.APT.2018.10.015.
7. Chaudhari, S.P.; Gupte, A. Mesoporous Silica as a Carrier for Amorphous Solid Dispersion. *Br. J. Pharm. Res.* **2017**, *16*, 1–19, doi:10.9734/BJPR/2017/33553.
8. Lombardo, R.; Musumeci, T.; Carbone, C.; Pignatello, R. Nanotechnologies for Intranasal Drug Delivery: An Update of Literature. **2021**, *26*, 824–845, doi:10.1080/10837450.2021.1950186.
9. Damier, P.; Hirsch, E.C.; Agid, Y.; Graybiel, A.M. The Substantia Nigra of the Human BrainII. Patterns of Loss of Dopamine-Containing Neurons in Parkinson's Disease. *Brain* **1999**, *122*, 1437–1448, doi:10.1093/BRAIN/122.8.1437.
10. Hallett, M. Parkinson's Disease Tremor: Pathophysiology. *Parkinsonism Relat. Disord.*

2012, *18*, S85–S86, doi:10.1016/S1353-8020(11)70027-X.

11. Pilleri, M.; Antonini, A. Novel Levodopa Formulations in the Treatment of Parkinson's Disease. **2014**, *14*, 143–149, doi:10.1586/14737175.2014.877840.
12. Haddad, F.; Sawalha, M.; Khawaja, Y.; Najjar, A.; Karaman, R. Dopamine and Levodopa Prodrugs for the Treatment of Parkinson's Disease. *Mol. 2018, Vol. 23, Page 40* **2017**, *23*, 40, doi:10.3390/MOLECULES23010040.
13. Jankovic, J.; Aguilar, L.G. Current Approaches to the Treatment of Parkinson's Disease. *Neuropsychiatr. Dis. Treat.* **2008**, *4*, 743, doi:10.2147/NDT.S2006.
14. Levodopa: Uses, Interactions, Mechanism of Action | DrugBank Online Available online: https://go.drugbank.com/drugs/DB01235 (accessed on 4 May 2022).
15. Thanvi, B.R.; Lo, T.C.N. Long Term Motor Complications of Levodopa: Clinical Features, Mechanisms, and Management Strategies. *Postgrad. Med. J.* **2004**, *80*, 452–458, doi:10.1136/PGMJ.2003.013912.
16. Stocchi, F.; Vacca, L.; Ruggieri, S.; Olanow, C.W. Intermittent vs Continuous Levodopa Administration in Patients With Advanced Parkinson Disease: A Clinical and Pharmacokinetic Study. *Arch. Neurol.* **2005**, *62*, 905–910, doi:10.1001/ARCHNEUR.62.6.905.
17. Westin, J.; Nyholm, D.; Pålhagen, S.; Willows, T.; Groth, T.; Dougherty, M.; Karlsson, M.O. A Pharmacokinetic-Pharmacodynamic Model for Duodenal Levodopa Infusion. *Clin. Neuropharmacol.* **2011**, *34*, 61–65, doi:10.1097/WNF.0B013E31820B570A.
18. Oakes, D.; Shoulson, I.; Kieburtz, K.; Rudolph, A.; Lang, A.; Western Hos-pital, T.; Warren Olanow, C.; Tanner, C. Levodopa and the Progression of Parkinson's Disease. **2009**, *351*, 2498–2508, doi:10.1056/NEJMOA033447.
19. Waiting for ON: A Major Problem in Patients With Parkinson D... : Clinical Neuropharmacology Available online: https://journals.lww.com/clinicalneuropharm/Fulltext/2003/07000/A_Home_Diary_to_Assess_Functional_Status_in.9.aspx (accessed on 4 May 2022).
20. Stocchi, F.; Marconi, S. Factors Associated with Motor Fluctuations and Dyskinesia in Parkinson Disease: Potential Role of a New Melevodopa plus Carbidopa Formulation (Sirio). *Clin. Neuropharmacol.* **2010**, *33*, 198–203, doi:10.1097/WNF.0B013E3181DE8924.
21. Safety, Tolerability and Levodopa Pharmacokinetics Following Inhaled Administration

of CVT-301, a Levodopa Dry Powder Aerosol, in Healthy, Adult Subjects | Health & Environmental Research Online (HERO) | US EPA Available online: https://hero.epa.gov/hero/index.cfm/reference/details/reference_id/2649749 (accessed on 4 May 2022).

22. You, H.; Mariani, L.L.; Mangone, G.; Le Febvre de Nailly, D.; Charbonnier-Beaupel, F.; Corvol, J.C. Molecular Basis of Dopamine Replacement Therapy and Its Side Effects in Parkinson's Disease. *Cell Tissue Res. 2018 3731* **2018**, *373*, 111–135, doi:10.1007/S00441-018-2813-2.
23. Parkinson's Disease | Teesneuro.Org Available online: https://teesneuro.org/specific-conditions/parkinsons-disease-and-pals/ (accessed on 4 May 2022).
24. Tambasco, N.; Romoli, M.; Calabresi, P. Levodopa in Parkinson's Disease: Current Status and Future Developments. *Curr. Neuropharmacol.* **2017**, *16*, 1239–1252, doi:10.2174/1570159X15666170510143821.
25. Nyholm, D.; Nilsson Remahl, A.I.M.; Dizdar, N.; Constantinescu, R.; Holmberg, B.; Jansson, R.; Aquilonius, S.M.; Askmark, H. Duodenal Levodopa Infusion Monotherapy vs Oral Polypharmacy in Advanced Parkinson Disease. *Neurology* **2005**, *64*, 216–223, doi:10.1212/01.WNL.0000149637.70961.4C.
26. Inbrija (Levodopa) FDA Approval History - Drugs.Com Available online: https://www.drugs.com/history/inbrija.html (accessed on 4 May 2022).
27. Inbrija | European Medicines Agency Available online: https://www.ema.europa.eu/en/medicines/human/EPAR/inbrija (accessed on 4 May 2022).
28. LeWitt, P.A.; Hauser, R.A.; Grosset, D.G.; Stocchi, F.; Saint-Hilaire, M.H.; Ellenbogen, A.; Leinonen, M.; Hampson, N.B.; DeFeo-Fraulini, T.; Freed, M.I.; et al. A Randomized Trial of Inhaled Levodopa (CVT-301) for Motor Fluctuations in Parkinson's Disease. *Mov. Disord.* **2016**, *31*, 1356–1365, doi:10.1002/MDS.26611.
29. Stocchi, F.; Fabbri, L.; Vecsei, L.; Krygowska-Wajs, A.; Monici Preti, P.A.; Ruggieri, S.A. Clinical Efficacy of a Single Afternoon Dose of Effervescent Levodopa-Carbidopa Preparation (CHF 1512) in Fluctuating Parkinson Disease. *Clin. Neuropharmacol.* **2007**, *30*, 18–24, doi:10.1097/01.WNF.0000236762.77913.C6.
30. Stocchi, F.; Barbato, L.; Bramante, L.; Bonamartini, A.; Ruggieri, S. The Clinical Efficacy of a Single Afternoon Dose of Levodopa Methyl Ester: A Double-Blind Cross-

over Study versus Placebo. *Funct. Neurol.* **1994**, *9*, 259–264.

31. Home - The Cambridge Crystallographic Data Centre (CCDC) Available online: https://www.ccdc.cam.ac.uk/ (accessed on 4 May 2022).
32. Stocchi, F.; Zappia, M.; Dall'Armi, V.; Kulisevsky, J.; Lamberti, P.; Obeso, J.A. Melevodopa/Carbidopa Effervescent Formulation in the Treatment of Motor Fluctuations in Advanced Parkinson's Disease. *Mov. Disord.* **2010**, *25*, 1881–1887, doi:10.1002/MDS.23206.
33. Lee, Y.H.; Kim, K.H.; Yoon, I.K.; Lee, K.E.; Chun, I.K.; Rhie, J.Y.; Gwak, H.S. Pharmacokinetic Evaluation of Formulated Levodopa Methyl Ester Nasal Delivery Systems. *Eur. J. Drug Metab. Pharmacokinet.* **2014**, *39*, 237–242, doi:10.1007/S13318-013-0171-8/TABLES/2.
34. Gizurarson, S. Anatomical and Histological Factors Affecting Intranasal Drug and Vaccine Delivery. *Curr. Drug Deliv.* **2012**, *9*, 566–582, doi:10.2174/156720112803529828.
35. Jadhav, K.; Gambhire, M.; Shaikh, I.; Kadam, V.; Pisal, S. Nasal Drug Delivery System-Factors Affecting and Applications. *Curr. Drug ther.* **2008**, *2*, 27–38, doi:10.2174/157488507779422374.
36. Hanson, L.R.; Frey, W.H. Intranasal Delivery Bypasses the Blood-Brain Barrier to Target Therapeutic Agents to the Central Nervous System and Treat Neurodegenerative Disease. *BMC Neurosci. 2008 93* **2008**, *9*, 1–4, doi:10.1186/1471-2202-9-S3-S5.
37. Davis, S.S.; Illum, L. Absorption Enhancers for Nasal Drug Delivery. *Clin. Pharmacokinet. 2003 4213* **2012**, *42*, 1107–1128, doi:10.2165/00003088-200342130-00003.
38. Scherließ, R. Nasal Formulations for Drug Administration and Characterization of Nasal Preparations in Drug Delivery. **2020**, *11*, 183–191, doi:10.4155/TDE-2019-0086.
39. Bitter, C.; Suter-Zimmermann, K.; Surber, C. Nasal Drug Delivery in Humans. *Top. Appl. Mucosa* **2011**, *40*, 20–35.
40. Ritthidej, G.C. Nasal Delivery of Peptides and Proteins with Chitosan and Related Mucoadhesive Polymers. *Pept. Protein Deliv.* **2011**, 47–68, doi:10.1016/B978-0-12-384935-9.10003-3.
41. Tiozzo Fasiolo, L.; Manniello, M.D.; Tratta, E.; Buttini, F.; Rossi, A.; Sonvico, F.; Bortolotti, F.; Russo, P.; Colombo, G. Opportunity and Challenges of Nasal Powders:

Drug Formulation and Delivery. *Eur. J. Pharm. Sci.* **2018**, *113*, 2–17, doi:10.1016/J.EJPS.2017.09.027.

42. "Drug-Excipient Compatibility Studies in Formulation Development: Curre" by Vivek S. Dave, Rahul V. Haware et Al. Available online: https://fisherpub.sjfc.edu/pharmacy_facpub/212/ (accessed on 4 May 2022).
43. Ledeti, I.; Bolintineanu, S.; Vlase, G.; Circioban, D.; Ledeti, A.; Vlase, T.; Suta, L.M.; Caunii, A.; Murariu, M. Compatibility Study between Antiparkinsonian Drug Levodopa and Excipients by FTIR Spectroscopy, X-Ray Diffraction and Thermal Analysis. *J. Therm. Anal. Calorim.* **2017**, *130*, 433–441, doi:10.1007/S10973-017-6393-2/TABLES/3.
44. Trenkel, M.; Scherließ, R. Nasal Powder Formulations: In-Vitro Characterisation of the Impact of Powders on Nasal Residence Time and Sensory Effects. *Pharm. 2021, Vol. 13, Page 385* **2021**, *13*, 385, doi:10.3390/PHARMACEUTICS13030385.
45. Pozzoli, M.; Rogueda, P.; Zhu, B.; Smith, T.; Young, P.M.; Traini, D.; Sonvico, F. Dry Powder Nasal Drug Delivery: Challenges, Opportunities and a Study of the Commercial Teijin Puvlizer Rhinocort Device and Formulation. **2016**, *42*, 1660–1668, doi:10.3109/03639045.2016.1160110.
46. Dexamethasone Cipecilate Available online: https://www.pharmacodia.com/yaodu/html/v1/chemicals/0771fc6f0f4b1d7d1bb73bbbe14e0e31.html (accessed on 4 May 2022).
47. Fda; Cder Rhinocort (Budesonide) Nasal Spray Label.
48. Pharmaceutical Quality of Inhalation and Nasal Products | European Medicines Agency Available online: https://www.ema.europa.eu/en/pharmaceutical-quality-inhalation-nasal-products (accessed on 4 May 2022).
49. US20030158206A1 - Intranasal Formulations for Treating Sexual Disorders - Google Patents Available online: https://patents.google.com/patent/US20030158206A1/en (accessed on 4 May 2022).
50. Freeze Drying / Lyophilization Information: Basic Principles Available online: https://www.spscientific.com/freeze-drying-lyophilization-basics/ (accessed on 4 May 2022).
51. Pilcer, G.; Amighi, K. Formulation Strategy and Use of Excipients in Pulmonary Drug Delivery. *Int. J. Pharm.* **2010**, *392*, 1–19, doi:10.1016/J.IJPHARM.2010.03.017.

52. Cho, W.; Kim, M.S.; Jung, M.S.; Park, J.; Cha, K.H.; Kim, J.S.; Park, H.J.; Alhalaweh, A.; Velaga, S.P.; Hwang, S.J. Design of Salmon Calcitonin Particles for Nasal Delivery Using Spray-Drying and Novel Supercritical Fluid-Assisted Spray-Drying Processes. *Int. J. Pharm.* **2015**, *478*, 288–296, doi:10.1016/J.IJPHARM.2014.11.051.
53. Garmise, R.J.; Staats, H.F.; Hickey, A.J. Novel Dry Powder Preparations of Whole Inactivated Influenza Virus for Nasal Vaccination. *AAPS PharmSciTech 2007 84* **2007**, *8*, 2–10, doi:10.1208/PT0804081.
54. Wang, S.H.; Kirwan, S.M.; Abraham, S.N.; Staats, H.F.; Hickey, A.J. Stable Dry Powder Formulation for Nasal Delivery of Anthrax Vaccine. *J. Pharm. Sci.* **2012**, *101*, 31–47, doi:10.1002/JPS.22742.
55. Balducci, A.G.; Ferraro, L.; Bortolotti, F.; Nastruzzi, C.; Colombo, P.; Sonvico, F.; Russo, P.; Colombo, G. Antidiuretic Effect of Desmopressin Chimera Agglomerates by Nasal Administration in Rats. *Int. J. Pharm.* **2013**, *440*, 154–160, doi:10.1016/J.IJPHARM.2012.09.049.
56. Russo, P.; Sacchetti, C.; Pasquali, I.; Bettini, R.; Massimo, G.; Colombo, P.; Rossi, A. Primary Microparticles and Agglomerates of Morphine for Nasal Insufflation. *J. Pharm. Sci.* **2006**, *95*, 2553–2561, doi:10.1002/JPS.20604.
57. Russo, P.; Buttini, F.; Sonvico, F.; Bettini, R.; Massimo, G.; Sacchetti, C.; Colombo, P.; Santi, P. Chimeral Agglomerates of Microparticles for the Administration of Caffeine Nasal Powders. *J. Drug Deliv. Sci. Technol.* **2004**, *14*, 449–454, doi:10.1016/S1773-2247(04)50083-7.
58. Barzegar-Jalali, M.; Valizadeh, H.; Shadbad, M.R.S.; Adibkia, K.; Mohammadi, G.; Farahani, A.; Arash, Z.; Nokhodchi, A. Cogrinding as an Approach to Enhance Dissolution Rate of a Poorly Water-Soluble Drug (Gliclazide). *Powder Technol.* **2010**, *197*, 150–158, doi:10.1016/J.POWTEC.2009.09.008.
59. ICH Q3C (R8) Residual Solvents | European Medicines Agency Available online: https://www.ema.europa.eu/en/ich-q3c-r8-residual-solvents (accessed on 4 May 2022).
60. Mio, H.; Kano, J.; Saito, F. Scale-up Method of Planetary Ball Mill. *Chem. Eng. Sci.* **2004**, *59*, 5909–5916, doi:10.1016/J.CES.2004.07.020.
61. Iwasaki, T.; Yabuuchi, T.; Nakagawa, H.; Watano, S. Scale-up Methodology for Tumbling Ball Mill Based on Impact Energy of Grinding Balls Using Discrete Element Analysis. *Adv. Powder Technol.* **2010**, *21*, 623–629, doi:10.1016/J.APT.2010.04.008.

62. Brime, B.; Ballesteros, M.P.; Frutos, P. Preparation and in Vitro Characterization of Gelatin Microspheres Containing Levodopa for Nasal Administration. **2008**, *17*, 777–784, doi:10.1080/02652040050161765.
63. Sharma, S.; Lohan, S.; Murthy, R.S.R. Formulation and Characterization of Intranasal Mucoadhesive Nanoparticulates and Thermo-Reversible Gel of Levodopa for Brain Delivery. **2014**, *40*, 869–878, doi:10.3109/03639045.2013.789051.
64. Alipour, S.; Azari, H.; Ahmadi, F. In Situ Thermosensitive Gel of Levodopa: Potential Formulation for Nose to Brain Delivery in Parkinson Disease. *Trends Pharm. Sci.* **2020**, *6*, 97–104, doi:10.30476/TIPS.2020.86526.1052.
65. Vasa, D.M.; Buckner, I.S.; Cavanaugh, J.E.; Wildfong, P.L.D. Improved Flux of Levodopa via Direct Deposition of Solid Microparticles on Nasal Tissue. *AAPS PharmSciTech* **2017**, *18*, 904–912, doi:10.1208/S12249-016-0581-4/FIGURES/8.
66. Kim, T.K.; Kang, W.; Chun, I.K.; Oh, S.Y.; Lee, Y.H.; Gwak, H.S. Pharmacokinetic Evaluation and Modeling of Formulated Levodopa Intranasal Delivery Systems. *Eur. J. Pharm. Sci.* **2009**, *38*, 525–532, doi:10.1016/J.EJPS.2009.09.019.
67. Chun, I.K.; Lee, Y.H.; Lee, K.E.; Gwak, H.S. Design and Evaluation of Levodopa Methyl Ester Intranasal Delivery Systems. *J. Parkinsons. Dis.* **2011**, *1*, 101–107, doi:10.3233/JPD-2011-10011.
68. Arts, J.H.E.; Muijser, H.; Duistermaat, E.; Junker, K.; Kuper, C.F. Five-Day Inhalation Toxicity Study of Three Types of Synthetic Amorphous Silicas in Wistar Rats and Post-Exposure Evaluations for up to 3 Months. *Food Chem. Toxicol.* **2007**, *45*, 1856–1867, doi:10.1016/J.FCT.2007.04.001.
69. Hamzehloo, M.; Karimi, J.; Aghapoor, K.; Sayahi, H.; Darabi, H.R. The Synergistic Cooperation between MCM-41 and Azithromycin: A PH Responsive System for Drug Adsorption and Release. *J. Porous Mater.* **2018**, *25*, 1275–1285, doi:10.1007/S10934-017-0538-3/TABLES/3.
70. Choudhari, Y.; Hoefer, H.; Libanati, C.; Monsuur, F.; McCarthy, W. Mesoporous Silica Drug Delivery Systems. **2014**, 665–693, doi:10.1007/978-1-4939-1598-9_23.
71. Vallet-Regí, M.; Balas, F.; Arcos, D. Mesoporous Materials for Drug Delivery. *Angew. Chemie Int. Ed.* **2007**, *46*, 7548–7558, doi:10.1002/ANIE.200604488.
72. Antonino, R.S.C.M.Q.; Ruggiero, M.; Song, Z.; Nascimento, T.L.; Lima, E.M.; Bohr, A.; Knopp, M.M.; Löbmann, K. Impact of Drug Loading in Mesoporous Silica-

Amorphous Formulations on the Physical Stability of Drugs with High Recrystallization Tendency. *Int. J. Pharm. X* **2019**, *1*, 100026, doi:10.1016/J.IJPX.2019.100026.

73. Bakhshian Nik, A.; Zare, H.; Razavi, S.; Mohammadi, H.; Torab Ahmadi, P.; Yazdani, N.; Bayandori, M.; Rabiee, N.; Izadi Mobarakeh, J. Smart Drug Delivery: Capping Strategies for Mesoporous Silica Nanoparticles. *Microporous Mesoporous Mater.* **2020**, *299*, 110115, doi:10.1016/J.MICROMESO.2020.110115.
74. Doadrio, J.C.; Sousa, E.M.B.; Izquierdo-Barba, I.; Doadrio, A.L.; Perez-Pariente, J.; Vallet-Regí, M. Functionalization of Mesoporous Materials with Long Alkyl Chains as a Strategy for Controlling Drug Delivery Pattern. *J. Mater. Chem.* **2006**, *16*, 462–466, doi:10.1039/B510101H.
75. Qu, F.; Zhu, G.; Huang, S.; Li, S.; Qiu, S. Effective Controlled Release of Captopril by Silylation of Mesoporous MCM-41. *ChemPhysChem* **2006**, *7*, 400–406, doi:10.1002/CPHC.200500294.
76. Tang, Q.; Xu, Y.; Wu, D.; Sun, Y. Hydrophobicity-Controlled Drug Delivery System from Organic Modified Mesoporous Silica. **2006**, *35*, 474–475, doi:10.1246/CL.2006.474.
77. Kinnari, P.; Mäkilä, E.; Heikkilä, T.; Salonen, J.; Hirvonen, J.; Santos, H.A. Comparison of Mesoporous Silicon and Non-Ordered Mesoporous Silica Materials as Drug Carriers for Itraconazole. *Int. J. Pharm.* **2011**, *414*, 148–156, doi:10.1016/J.IJPHARM.2011.05.021.
78. Benali, M.; Aillet, T.; Saleh, K. Effect of Operating Conditions on the Hydrophobisation of Silica-Based Porous Particles in a Fluidised-Bed Reactor: Temperature Effect. *Adv. Powder Technol.* **2012**, *23*, 596–600, doi:10.1016/J.APT.2011.06.007.
79. Limnell, T.; Santos, H.A.; Mäkilä, E.; Heikkilä, T.; Salonen, J.; Murzin, D.Y.; Kumar, N.; Laaksonen, T.; Peltonen, L.; Hirvonen, J. Drug Delivery Formulations of Ordered and Nonordered Mesoporous Silica: Comparison of Three Drug Loading Methods. *J. Pharm. Sci.* **2011**, *100*, 3294–3306, doi:10.1002/JPS.22577.
80. Heikkilä, T.; Salonen, J.; Tuura, J.; Kumar, N.; Salmi, T.; Murzin, D.Y.; Hamdy, M.S.; Mul, G.; Laitinen, L.; Kaukonen, A.M.; et al. Evaluation of Mesoporous TCPSi, MCM-41, SBA-15, and TUD-1 Materials as API Carriers for Oral Drug Delivery. **2008**, *14*, 337–347, doi:10.1080/10717540601098823.
81. Waters, L.J.; Hanrahan, J.P.; Tobin, J.M.; Finch, C. V.; Parkes, G.M.B.; Ahmad, S.A.;

Mohammad, F.; Saleem, M. Enhancing the Dissolution of Phenylbutazone Using Syloid® Based Mesoporous Silicas for Oral Equine Applications. *J. Pharm. Anal.* **2018**, *8*, 181–186, doi:10.1016/J.JPHA.2018.01.004.

82. Protsak, I.S.; Gun'Ko, V.M.; Henderson, I.M.; Pakhlov, E.M.; Sternik, D.; Le, Z. Nanostructured Amorphous Silicas Hydrophobized by Various Pathways. *ACS Omega* **2019**, *4*, 13863–13871, doi:10.1021/ACSOMEGA.9B01508/SUPPL_FILE/AO9B01508_SI_001.PDF.
83. Xu, W.; Riikonen, J.; Lehto, V.P. Mesoporous Systems for Poorly Soluble Drugs. *Int. J. Pharm.* **2013**, *453*, 181–197, doi:10.1016/J.IJPHARM.2012.09.008.
84. Maleki, A.; Kettiger, H.; Schoubben, A.; Rosenholm, J.M.; Ambrogi, V.; Hamidi, M. Mesoporous Silica Materials: From Physico-Chemical Properties to Enhanced Dissolution of Poorly Water-Soluble Drugs. *J. Control. Release* **2017**, *262*, 329–347, doi:10.1016/J.JCONREL.2017.07.047.
85. Mitran, R.A.; Matei, C.; Berger, D.; Băjenaru, L.; Moisescu, M.G. Controlling Drug Release from Mesoporous Silica through an Amorphous, Nanoconfined 1-Tetradecanol Layer. *Eur. J. Pharm. Biopharm.* **2018**, *127*, 318–325, doi:10.1016/J.EJPB.2018.02.020.
86. Grace Materials Technologies Grace Materials Technologies. Safety Data Sheet of SYLOID® 244 Available online: https://www.medisca.com/NDC_SPECS/MUS/3089/MSDS/3089.pdf (accessed on 4 May 2022).
87. Beg, S.; Hasnain, M.S.; Rahman, M.; Swain, S. Introduction to Quality by Design (QbD): Fundamentals, Principles, and Applications. *Pharm. Qual. by Des. Princ. Appl.* **2019**, 1–17, doi:10.1016/B978-0-12-815799-2.00001-0.
88. Yu, L.X. Pharmaceutical Quality by Design: Product and Process Development, Understanding, and Control. *Pharm. Res.* **2008**, *25*, 781–791, doi:10.1007/S11095-007-9511-1/TABLES/2.
89. J. M. Juran *Juran on Quality by Design: The New Steps for Planning Quality Into Goods ... - J. M. Juran, JOSEPH M AUTOR JURAN - Google Könyvek*;
90. ICH Q8 (R2) Pharmaceutical Development | European Medicines Agency Available online: https://www.ema.europa.eu/en/ich-q8-r2-pharmaceutical-development (accessed on 4 May 2022).
91. ICH Q9 Quality Risk Management | European Medicines Agency Available online:

https://www.ema.europa.eu/en/ich-q9-quality-risk-management (accessed on 4 May 2022).

92. ICH Q10 Pharmaceutical Quality System | European Medicines Agency Available online: https://www.ema.europa.eu/en/ich-q10-pharmaceutical-quality-system (accessed on 4 May 2022).
93. Pappert, E.J.; Buhrfiend, C.; Lipton, J.W.; Carvey, P.M.; Stebbins, G.T.; Goetz, C.G. Levodopa Stability in Solution: Time Course, Environmental Effects, and Practical Recommendations for Clinical Use. *Mov. Disord.* **1996**, *11*, 24–26, doi:10.1002/MDS.870110106.
94. Scaturro, A.L.; De Caro, V.; Campisi, G.; Giannola, L.I. Potential Transbuccal Delivery of L-DOPA Methylester Prodrug: Stability in the Environment of the Oral Cavity and Ability to Cross the Mucosal Tissue. **2014**, *23*, 2355–2362, doi:10.3109/10717544.2014.987332.
95. Kiss, T.; Katona, G.; Ambrus, R. Crystallization and Physicochemical Investigation of Melevodopa Hydrochloride, a Commercially Available Antiparkinsonian Active Substance. *Acta Pharm. Hung.* **2021**, *91*, 45–52, doi:10.33892/APH.2021.91.45-52.
96. Isariebel, Q.P.; Carine, J.L.; Ulises-Javier, J.H.; Anne-Marie, W.; Henri, D. Sonolysis of Levodopa and Paracetamol in Aqueous Solutions. *Ultrason. Sonochem.* **2009**, *16*, 610–616, doi:10.1016/J.ULTSONCH.2008.11.008.
97. LabNetwork - [(2S)-3-(3,4-Dihydroxyphenyl)-1-Methoxy-1-Oxopropan-2-Yl]Azanium;Chloride Available online: https://www.labnetwork.com/frontend-app/p/#!/moleculedetails/LN00194262 (accessed on 4 May 2022).
98. Lewitt, P.A.; Library, W.O. Levodopa Therapy for Parkinson's Disease: Pharmacokinetics and Pharmacodynamics. *Mov. Disord.* **2015**, *30*, 64–72, doi:10.1002/MDS.26082.
99. Shim, S.; Yoo, H.S. The Application of Mucoadhesive Chitosan Nanoparticles in Nasal Drug Delivery. *Mar. Drugs 2020, Vol. 18, Page 605* **2020**, *18*, 605, doi:10.3390/MD18120605.
100. Casettari, L.; Illum, L. Chitosan in Nasal Delivery Systems for Therapeutic Drugs. *J. Control. Release* **2014**, *190*, 189–200, doi:10.1016/J.JCONREL.2014.05.003.
101. Horvát, S.; Fehér, A.; Wolburg, H.; Sipos, P.; Veszelka, S.; Tóth, A.; Kis, L.; Kurunczi, A.; Balogh, G.; Kürti, L.; et al. Sodium Hyaluronate as a Mucoadhesive Component in

Nasal Formulation Enhances Delivery of Molecules to Brain Tissue. *Eur. J. Pharm. Biopharm.* **2009**, *72*, 252–259, doi:10.1016/J.EJPB.2008.10.009.

102. Giuliani, A.; Balducci, A.G.; Zironi, E.; Colombo, G.; Bortolotti, F.; Lorenzini, L.; Galligioni, V.; Pagliuca, G.; Scagliarini, A.; Calzà, L.; et al. In Vivo Nose-to-Brain Delivery of the Hydrophilic Antiviral Ribavirin by Microparticle Agglomerates. *Drug Deliv.* **2018**, *25*, 376–387, doi:10.1080/10717544.2018.1428242/SUPPL_FILE/IDRD_A_1428242_SM7572.DOCX.
103. Rassu, G.; Sorrenti, M.; Catenacci, L.; Pavan, B.; Ferraro, L.; Gavini, E.; Bonferoni, M.C.; Giunchedi, P.; Dalpiaz, A. Versatile Nasal Application of Cyclodextrins: Excipients and/or Actives? *Pharm. 2021, Vol. 13, Page 1180* **2021**, *13*, 1180, doi:10.3390/PHARMACEUTICS13081180.
104. Jain, S.A.; Chauk, D.S.; Mahajan, H.S.; Tekade, A.R.; Gattani, S.G. Formulation and Evaluation of Nasal Mucoadhesive Microspheres of Sumatriptan Succinate. **2009**, *26*, 711–721, doi:10.3109/02652040802685241.
105. Ogawa, K.; Uchida, M.; Yamaki, T.; Matsuzaki, H.; Kimura, M.; Okazaki, M.; Uchida, H.; Natsume, H. Delivery of Acetaminophen to the Central Nervous System and the Pharmacological Effect after Intranasal Administration with a Mucoadhesive Agent and Absorption Enhancer. *Int. J. Pharm.* **2021**, *594*, 120046, doi:10.1016/J.IJPHARM.2020.120046.
106. Varga, P.; Ambrus, R.; Szabó-Révész, P.; Kókai, D.; Burián, K.; Bella, Z.; Fenyvesi, F.; Bartos, C. Physico-Chemical, In Vitro and Ex Vivo Characterization of Meloxicam Potassium-Cyclodextrin Nanospheres. *Pharm. 2021, Vol. 13, Page 1883* **2021**, *13*, 1883, doi:10.3390/PHARMACEUTICS13111883.
107. Buchanan, R.L.; Bagi, L.K. Effect of Water Activity and Humectant Identity on the Growth Kinetics OfEscherichia ColiO157:H7. *Food Microbiol.* **1997**, *14*, 413–423, doi:10.1006/FMIC.1997.0101.
108. Pallagi, E.; Ambrus, R.; Szabó-Révész, P.; Csóka, I. Adaptation of the Quality by Design Concept in Early Pharmaceutical Development of an Intranasal Nanosized Formulation. *Int. J. Pharm.* **2015**, *491*, 384–392, doi:10.1016/J.IJPHARM.2015.06.018.
109. Chudiwal, S.S.; Dehghan, M.H.G. Quality by Design Approach for Development of Suspension Nasal Spray Products: A Case Study on Budesonide Nasal Suspension. **2016**,

42, 1643–1652, doi:10.3109/03639045.2016.1160108.

110. Narendar, D.; Arjun, N.; Someshwar, K.; Madhusudan Rao, Y. Quality by Design Approach for Development and Optimization of Quetiapine Fumarate Effervescent Floating Matrix Tablets for Improved Oral Bioavailability. *J. Pharm. Investig.* **2016**, *46*, 253–263, doi:10.1007/S40005-016-0232-5/TABLES/7.
111. Park, S.Y.; Kang, Z.; Thapa, P.; Jin, Y.S.; Park, J.W.; Lim, H.J.; Lee, J.Y.; Lee, S.W.; Seo, M.H.; Kim, M.S.; et al. Development of Sorafenib Loaded Nanoparticles to Improve Oral Bioavailability Using a Quality by Design Approach. *Int. J. Pharm.* **2019**, *566*, 229–238, doi:10.1016/J.IJPHARM.2019.05.064.
112. Wang, L.; Urata, C.; Sato, T.; England, M.W.; Hozumi, A. Self-Healing Superhydrophobic Materials Showing Quick Damage Recovery and Long-Term Durability. *Langmuir* **2017**, *33*, 9972–9978, doi:10.1021/ACS.LANGMUIR.7B02343/SUPPL_FILE/LA7B02343_SI_004.MOV.
113. Trivedi, V.; Bhomia, R.; Mitchell, J.C. Myristic Acid Coated Protein Immobilised Mesoporous Silica Particles as PH Induced Oral Delivery System for the Delivery of Biomolecules. *Pharm. 2019, Vol. 12, Page 153* **2019**, *12*, 153, doi:10.3390/PH12040153.
114. Paarakh, M.; Jose, P.; … C.S.-I.J.P.R.; 2018, undefined Release Kinetics–Concepts and Applications. *researchgate.net*.
115. Fernández-Colino, A.; Bermudez, J.M.; Arias, F.J.; Quinteros, D.; Gonzo, E. Development of a Mechanism and an Accurate and Simple Mathematical Model for the Description of Drug Release: Application to a Relevant Example of Acetazolamide-Controlled Release from a Bio-Inspired Elastin-Based Hydrogel. *Mater. Sci. Eng. C* **2016**, *61*, 286–292, doi:10.1016/J.MSEC.2015.12.050.
116. Suvakanta Dash; Padala Narasimha Murthy; Lilakanta Nath; Prasanta Chowdhury Kinetic Modeling on Drug Release from Controlled Drug Delivery Systems.
117. Gohel, M.C.; Sarvaiya, K.G.; Shah, A.R.; Brahmbhatt, B.K. Mathematical Approach for the Assessment of Similarity Factor Using a New Scheme for Calculating Weight. *Indian J. Pharm. Sci.* **2009**, *71*, 142, doi:10.4103/0250-474X.54281.
118. Santos Júnior, A.F.; de Freitas Santos Júnior, A.; Santos Barbosa, I.; Lima dos Santos, V.; Leal Silva, R.; Caetite Junior, E.; Barbosa, I.S.; Santos, V.L.; Silva, R.L.; Caetite Junior, E. Test of Dissolution and Comparison of in Vitro Dissolution Profiles of Coated

Ranitidine Tablets Marketed in Bahia, Brazil. *Brazilian J. Pharm. Sci.* **2014**, *50*, 83–89, doi:10.1590/S1984-82502011000100008.

119. ICH Q1A (R2) Stability Testing of New Drug Substances and Drug Products | European Medicines Agency Available online: https://www.ema.europa.eu/en/ich-q1a-r2-stability-testing-new-drug-substances-drug-products (accessed on 4 May 2022).
120. Edwin, B.; Hubert Joe, I. Vibrational Spectral Analysis of Anti-Neurodegenerative Drug Levodopa: A DFT Study. *J. Mol. Struct.* **2013**, *1034*, 119–127, doi:10.1016/J.MOLSTRUC.2012.09.004.
121. Musić, S.; Filipović-Vinceković, N.; Sekovanić, L. Precipitation of Amorphous SiO2 Particles and Their Properties. *28*, 89–94.
122. Roy Anderson; Jonathan Goff; Aki Imamura; Ed Kimble; Gabrielle Lockwood; Janis Matisons; Youlin Pan; Martin Reinert Silicon Compounds: Silanes and Silicones. **2013**, 547–1015.
123. Capel-Sanchez, M.C.; Barrio, L.; Campos-Martin, J.M.; Fierro, J.L.G. Silylation and Surface Properties of Chemically Grafted Hydrophobic Silica. *J. Colloid Interface Sci.* **2004**, *277*, 146–153, doi:10.1016/J.JCIS.2004.04.055.
124. Antonini, A.; Isaias, I.U.; Canesi, M.; Zibetti, M.; Mancini, F.; Manfredi, L.; Dal Fante, M.; Lopiano, L.; Pezzoli, G. Duodenal Levodopa Infusion for Advanced Parkinson's Disease: 12-Month Treatment Outcome. *Mov. Disord.* **2007**, *22*, 1145–1149, doi:10.1002/MDS.21500.

ACKNOWLEDGEMENTS

This work was supported by the Gedeon Richter Ltd – GINOP project (2.2.1-15-2016-00007), the ÚNKP-17-4-I-SZTE-3 New National Excellence Program of the Ministry of Human Capacities, the ÚNKP-20-3- SZTE-316 New National Excellence Program of the Ministry for Innovation and Technology from the source of The National Research Development and Innovation Fund, the Gedeon Richter's Centenary Foundation (Budapest) and the Hungarian Scientific Research Fund (OTKA) K134334.

The Ministry of Human Capacities, Hungary grant 20391-3/2018/FEKUSTRAT, EFOP 3.6.3-VEKOP-16-2017-00009 project, the Ministry of Human Capacities, Hungary (grant TKP-2020), as well as the GINOP-2.3.2.-15-2016-00060 and the GINOP-2.2.1-15-2016-00007 projects, are also acknowledged. The Syloid® XDP 3050 was kindly provided by Grace Materials Technologies (Grace GmbH, Worms, Germany).

I would like to thank **Prof. Dr. Piroska Szabó-Révész** for the scientifical mentoring and that she allowed me to join the research group as an M.Sc. student. Besides, I am grateful to **Prof. Dr. Ildikó Csóka** for providing us with the quality conditions to work as Ph.D. students at the Institute of Pharmaceutical Technology and Regulatory Affairs.

I am grateful to my supervisors, **Dr. habil Rita Ambrus Ph.D.** and **Dr. Gábor Katona Ph.D.** as well as to my co-authors for their support, thanks to which I could develop humanly and professionally throughout my Ph.D. studies. Among the co-authors, I would like to thank in particular our cooperation partners, **Dr. László Janovák Ph.D.** and **Prof. Dr. Eva Roblegg Ph.D.** who allowed me to work in their laboratory, directly with their research group. I am also grateful for the huge amount of help I got from the assistants from whom I would like to highlight **Piroska Lakatos-Fekete** who always made my tasks easier with her selfless help.

I am especially grateful to **my family, friends** and **girlfriend**, **Dr. Patrícia Varga** for their steady love and support during my studies which allow me to perform during my studies like this.